A Survey on Knot Traces

Yikai Teng

Born 07.04.2000 in Shanghai, China

28.06.2023

Master's Thesis Mathematics

Advisor: Dr. Arunima Ray

Second Advisor: Prof. Dr. Peter Teichner

Mathematisches Institut

Contents

Chapter 1

Introduction

Chapter 2

Knot Traces

A knot n-trace $X_n(K)$ is the 4-manifold with a single 2-handle glued to a 0-handle along the knot K, with framing coefficient n. Its boundary turns out to be the n-surgery of the 3-sphere along the knot K, $S_n^3(K)$.

In generic cases, two knot traces $X_n(K)$ and $X_n(K')$ are not homeomorphic since they have different boundaries. However, since there exist distinct knots K and K' that has homeomorphic n-surgeries, the corresponding n-traces are *a priori* not distinguishable. The goal of this chapter is to study the behaviour of such pairs of knot traces with homeomorphic boundaries.

In most part of this survey, we restrict our attention to 0-surgeries $S_0^3(K)$ and 0-traces $X_0(K)$.

2.1 Zero Surgery of a Knot

To begin with, there are a few known ways to construct prospectively distinct knot traces with homeomorphic 0-surgeries. We follow the historic order and introduce dualisable patters [4], annulus twisting [35], and RBG constructions [27].

2.1.1 Dualisable Patterns

The construction of dualisable patterns was first introduced by Brakes in 1980 [4]. However, in most of this section we will follow [26] for a more modern organisation.

A pattern $P : S^1 \hookrightarrow V$ is an oriented knot in the standard solid torus. Then, define μ_P and μ_V to be the positively oriented meridians for P (i.e. with linking number $+1$) and for V (i.e. homologous to a positive multiple

of μ_P) respectively. Further more, define λ_V to be $S^1 \times \{*\}$ oriented such that P is homologous to $n \cdot \lambda_V$, in which n is positive and is called the winding number of P. Finally define λ_P to be a framing curve of P that is homologous to a positive multiple of λ_V in $V \backslash \nu(P)$.

Under this definition, we can define a dualisable pattern.

Definition 2.1. A pattern P in a solid torus V is said to be dualisable if there exists a dual pattern P^* in a solid torus V^* such that there is an orientation preserving homeomorphism $f : V \backslash P \to V^* \backslash P^*$ with $f(\lambda_V) = \lambda_{P^*}, f(\lambda_P) = \lambda_{V^*}, f(\mu_V) = -\mu_{P^*}, f(\mu_P) = -\mu_{V^*}$.

Note that this definition is redundant. If we require only $f(\lambda_P = \lambda_{V^*})$ and $f(\mu_V) = -\mu_{P^*}$, we automatically have the whole definition by simply isotoping f in a small collar near the boundary.

There is also an alternate definition.

We start with the following observation. If we start with an embedding $i : S^1 \times D^2 \hookrightarrow S^1 \times S^2$ given by $(t, d) \mapsto (t, \iota(d))$ where $\iota : D^2 \hookrightarrow S^2$ is an orientation-preserving embedding, we can refine a pattern $P : S^1 \hookrightarrow S^1 \times D^2$ to a knot $\widehat{P}$ in $S^1 \times S^2$ by composing with the embedding i.

Definition 2.2. A pattern P is dualisable if the knot $\widehat{P}$ is isotopic to $\widehat{\lambda_V}$ in $S^1 \times S^2$. Here $\widehat{\lambda_V}$ is the knot given by the constructions above, treating λ_V as a pattern.

Lemma 2.3 (Proposition 3.5 of [26]). *The two definitions above are equivalent.*

Proof. For one direction, if the knot $\widehat{P}$ is isotopic to $\widehat{\lambda_V}$ in $S^1 \times S^2$, the complement $V^* := S^1 \times S^2 \backslash \nu(\widehat{P})$ is a solid torus. Now define the dual pattern $P^* := \widehat{\lambda_V}$ in V^*. Then μ_V is identified with $-\mu_{P^*}$ and λ_P with λ_{V^*}. Recall that these two identifications are enough to show that P and P^* are dual to each other in the first definition.

For the other direction, since μ_V is identified with $-\mu_{P*}$, the Dehn filling of $V^* \backslash \nu(P^*)$ along $-\mu_{P*}$ is diffeomprphic to the Dehn filling of $V \backslash \nu(P)$ along μ_V, which is diffeomorphic to $S^1 \times S^2 \backslash \nu(\widehat{P})$. Thus the tubular neighbourhoods of both $\widehat{P}$ and $\widehat{\lambda_V}$ gives two genus one Heegaard splittings of $S^1 \times S^2$. Thus $\widehat{P}$ is isotopic to $\pm\widehat{\lambda_V}$ since the genus one Heegaard splittings of $S^1 \times S^2$ is unique up to isotopy [45]. The claim on orientation immediately follows from $\widehat{P}$ being homologous to a positive multiple of λ_V in the first definition. $\square$

The two patterns described in Figure 2.1 give an example of a pair of dualisable patterns. Here the -4 means a twist box with 4 negative twists.
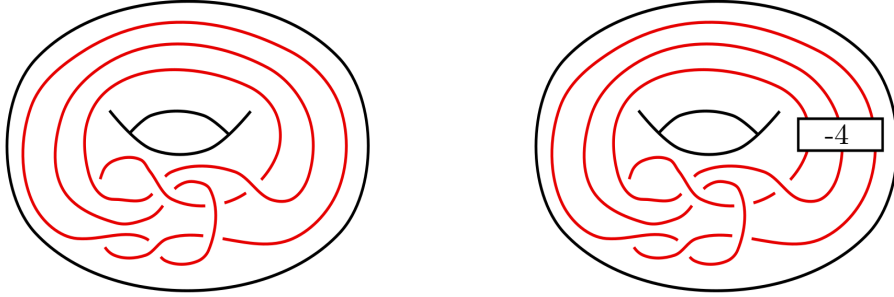

Figure 2.1: An example of a pair of dualisable patterns

It is proved in [4] that any pair of dualisable patterns create a pair of knots with homeomorphic zero-surgeries.

Theorem 2.4 (Theorem 1 of [4] and Theorem 3.8 of [26]). *If P is a dualisable pattern with dual P^*, then there is a 0-surgery homeomorphism $\phi : S_0^3(P(U)) \to S_0^3(P^*(U))$.*

Proof. Notice that $S_0^3(P(U))$ is the Dehn filling of $V \backslash \nu(P)$ along λ_P and λ_V, which by the first definition of dualisable patterns, is diffeomorphic to the Dehn filling of $V^* \backslash \nu(P^*)$ along λ_{V^*} and λ_{P^*}, which is exactly $S_0^3(P^*(U))$. This proves the theorem. $\square$

We also remark that the above construction can be generalised to non-zero knot surgery using Brakes' original formulation [4]. The statement is as follows.

Definition 2.5. Fix an unknot $U \subset S^3$. A knot $K \subset S^3 \backslash U$ is said to be trivilisable by a (q, n) twist if the linking number $lk(K, U) = n$ and the image of K under the Rolfsen twist $S^3 \cong S_{1/q}^3(U)$ is unknotted.

Theorem 2.6 (Theorem 1 of [4]). *For $i = 1$ and 2, if two knots K_i can be trivialised by a (q_i, n_i) twist, then we have a surgery homoemorphism the $(1 - N)/q_2$-surgery along a satellite of K_1 and the $(1 - N)/q_1$-surgery along a satellite of K_2, where $N = n_1^2 n_2^2 q_1 q_2$.*

Proof. See Theorem 1 of [4]. $\square$

Note that if we take n_i and q_i as 1, then we have exactly the statements about 0-surgeries above.

2.1.2 Annulus Twisting

Annulus twisting is a method invented by Osoinach [35] to construct an infinite family of knots with diffeomorphic 0-surgeries.

   We start by observing the following lemma about the k-twisted annulus A in the standardly embedded torus V shown in Figure 2.2.
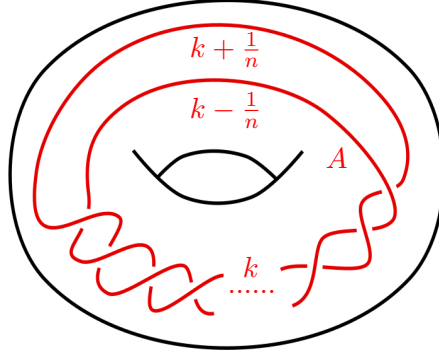

Figure 2.2: A k-twisted annulus in the standardly embedded solid torus

Lemma 2.7 (Theorem 2.1 and Corollary 2.2 of [35]). *If we do an $(k+1/n)$ surgery on one boundary component of A and $(k-1/n)$ surgery on the other, the resulting three manifold is still a solid torus V'. Moreover, any meridian for V is a meridian for V'.*

Proof. We show this by constructing a disk in $D' \subset V'$ as the image of a meridian disk $D \subset V$, and extending this homeomorphism to all of V'.

   The two pictures of Figure 2.3 depicts the meridian disk $D \subset V$ and D cutting out a tubular neighbourhood of the annulus A. We can fill in part of the boundary with a disk $\Delta \subset V \backslash D$ that passes through the cut out part n times, as depicted in Figure 2.4. The resulting surface is a twice punctured disk which can be capped off by $k \pm 1/n$ curves on tubular neighbourhoods of ∂A. This process yields the disk $D' \subset V'$.
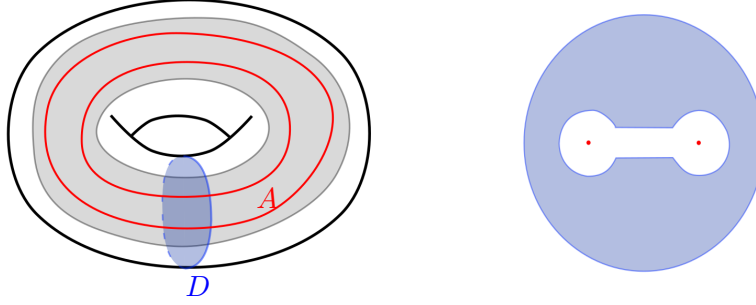
Figure 2.3: Left: Solid torus with the embedded annulus and meridian disk visible. Right: Meridian disk with the tubular neighbourhood of the annulus drilled out.
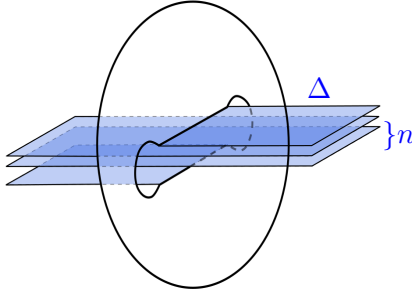
Figure 2.4: A filling of the drilled out neighbourhood.

This homeomorphism between V and V' is constructed exactly by mapping each meridian disk $D \times \{*\}$ to $D' \times \{*\}$. This construction automatically forces the identification of meridians of V and V'.

$\square$

With the above observation, we know that for an embedded annulus A in some 3-manifold M, there are infinitely many pairs of surgery on ∂A that does not change the homeomorphism type of M. Denote this operation "twisting along A n times".

Now we start with a k-twisted annulus A, and we do a band sum of the two boundary components to form a knot $K \subset S^3$. If we twist along the annulus A. we have an infinite family of knots $\{K_n\}$, as described by Figure 2.5.

Figure 2.5: A band sum the two boundary components of the annulus gives a knot

Doing a 0-surgery along the knot K corresponds to some r_n-surgery on the knot K_n. However, since by deqfinition it is required that $H_1(S_0^3(K)) \cong H_1(S_{0,1/n,-1/n}^3(K,l_1,l_2)) \cong H_1(S_{r_n}^3(K_n)) \cong \mathbb{Z}$, we can conclude that every $r_n = 0$.

Thus we have an infinite family of knots with homeomorphic 0-surgeries $\{K_n\}$.
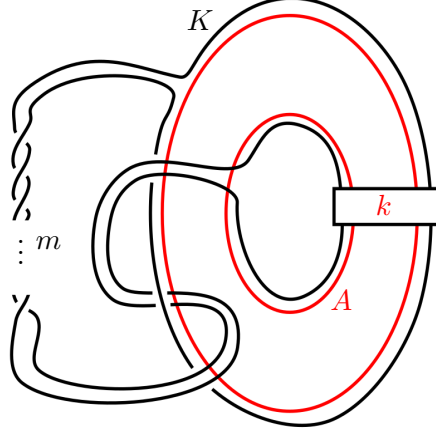
2.1.3 RBG Constructions

Finally, we consider RGB construction, which is a method developed by Manolescu and Piccirillo [27] that can completely represent 0-surgery homeomorphisms. This is given by Lemma 2.11 below.

Definition 2.8. An RBG-link is a 3-component framed link $L = (R,r) \cup (B,b) \cup (G,g) \subset S^3$ such that there are homeomorphisms $\psi_G : S_{r,b}^3(R \cup B) \to S^3$ and $\psi_B : S_{r,g}^3(R \cup G) \to S^3$, and $H_1(S_{r,b,g}^3(R \cup B \cup G); \mathbb{Z}) \cong \mathbb{Z}$.

For simplicity in later parts of this section, we consider a smaller family of RBG links, called the special RBG links.

Definition 2.9. An RBG link is called special if $b = g = 0$, and there are link isotopies $R \cup B \cong R \cup \mu_R \cong R \cup G$, where μ_R denotes the meridian of R.

Note that for general RBG links, it is in general very hard to obtain the associated knots K_B and K_G. However, for a special RBG link, we can

9

easily perform handle slides and slam-dunk homeomorphisms to obtain the associated knots.

Figuers 2.6 and 2.7 give two examples of RBG links. The first one is special while the second one is not.
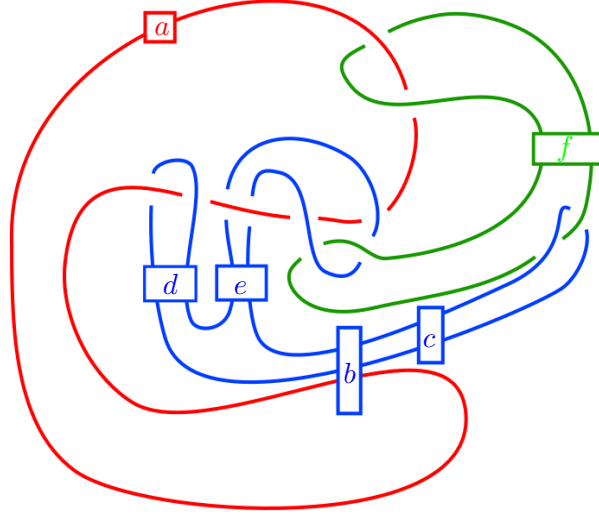

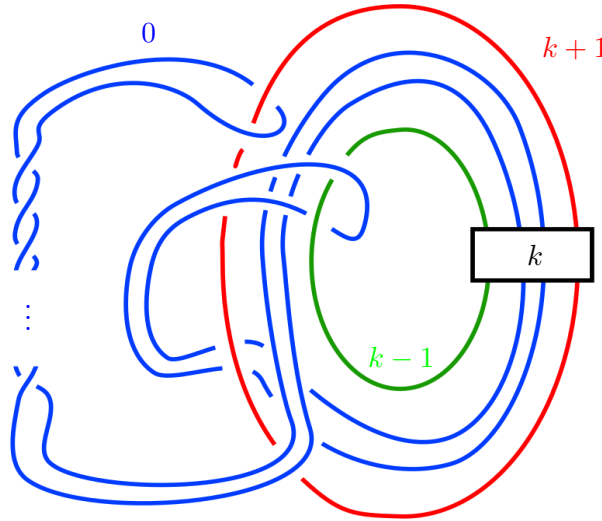Figure 2.6: A family of examples of special RBG links

Figure 2.7: A family of examples of non-special RBG links

The RBG link in Figure 2.6 defines the Manolescu-Piccirillo family of RBG links [27], which plays an important role in the following sections, so we will come back to that later. The RBG link in Figure 2.7 actually records a family of annulus twisting homeomorphisms, which we will discuss more in detail later in this section.

An RBG link is used to represent a 0-surgery homeomorphism. This is given by the following lemma/definition.

Lemma 2.10 (Theorem 1.2 of [27]). *Given an RBG link, there exist associated knots K_B and K_G and a homeomorphism $\phi_L : S_0^3(K_B) \to S_0^3(K_G)$.*

Proof. Since $S_{r,g}^3(R \cup G)$ is homeomorphic to S^3 by definition, we can define K_B to be the knot satisfying the homeomorphism $S_{r,*,g}^3(R \cup B \cup G) \to S_*^3(K_B)$. Here the framing $*$ denotes that we drill out the tubular neighbourhood of the knot and leave the cusp unfilled. Thus we can find a framing f_b such that we have the homeomorphism $\psi_B : S_{r,b,g}^3(R \cup B \cup G) \to S_{f_b}^3(K_B)$. Since we require $H_1(S_{r,b,g}^3(R \cup B \cup G); \mathbb{Z}) \cong \mathbb{Z}$ in the definition, we know that the framing $f_b = 0$.

Similarly, we can define the knot K_G to be the knot satisfying the homeomorphism $S_{r,b,*}^3(R \cup B \cup G) \to S_*^3(K_G)$, and have a homeomorphism $\psi_G : S_{r,b,g}^3(R \cup B \cup G) \to S_0^3(K_G)$.

The composition $\psi_B \circ \psi_G^{-1}$ gives the associated homeomorphism ϕ_L. $\square$

The converse of this lemma is also true:

Lemma 2.11 (Theorem 1.2 of [27]). *For every 0-surgery homeomorphism $\phi : S_0^3(K) \to S_0^3(K')$, there is an RBG link L such that f is its associated 0-surgery homeomorphism.*

Proof. Define (B, b) to be $(K, 0)$. Define $(R, r) := \phi((\mu_K, 0))$ to be the image of the 0-framed meridian B under the homeomorphism ϕ. Finally define $(G, g) := (\mu_R, 0)$ to be the 0-framed meridian of R. Together, this defines an RBG link L.

Indeed, there is a homeomorphism $S_{0,r}^3(B \cup R) \cong S_{0,0}^3(K, \mu_K)\S^3$, where the first map is the given homeomorphism ϕ, and the second a slam-dunk homeomorphism. Also, there is a slam-dunk homeomorphism $S_{r,0}^3(R, B) \cong S^3$. The homology requirement immediately follows. Thus L is indeed an RBG link. $\square$

Note that the RBG link constructed in this method is never special as long as K is non-trivial.

Also note that the assignment given in this lemma is not unique. A first example is to start with a special RBG link, and apply the above two lemmas to get a non-special RBG link.

The above two lemmas show that the set of all RBG links completely describes all 0-surgery homeomorphims. However, general RBG links are hard to deal with, and thus we will consider other constructions as well.

Before moving on, it is worth to study how RBG links would depict dualisable pattern and annulus twisting constructions. To see this, we need the following lemma.

Lemma 2.12 (Theorem 7.1 of [27]). *Fix an RBG link L with associated knots K_B, K_G. If we do a number of slides of B (resp. G) over R to get a new framed link L', then L' is also an RBG link, with its associated knots K_B', K_G' pair isotopic to the original associated knots K_B, K_G.*

Proof. We only prove the statement about sliding B over R thanks to symmetry of RBG links. Denote the new blue knot (B', b').

Note that the components R and G are left unchanged. Thus to check that the link L is still and RBG link, we need to check that S^3 surgered along R and B', which is immediate since handle slides do not change the homeomorphism type after the surgery. For the exact same reason, the homology condition still holds.

To check that $K_B \cong K_B'$, we construct a homeomorphism $S_0^3(K_B) \cong S_0^3(K_B')$ taking a zero framed meridian to a zero framed meridian. This homeomorphism can be taken to be the composition $\psi_{B'} \circ f \circ (\psi_B)^{-1} : S_0^3(K_B) \to S_{r,b,g}^3(R \cup B \cup G) \to S_{r,b',g}^3(R \cup B' \cup G) \to S_0^3(K_B')$, where the map f records the sliding homeomorphism. By chasing the zero framed meridian, it is easy to see that the constructed map satisfies the required conditions.

By excising the zero framed meridians, the constructed map restricts to a map $S^3 \backslash \nu(K_B) \to S^3 \backslash \nu(K_B')$ taking meridians to meridians, and thus extending to a knot equivalence $(S^3, K_B) \to (S^3, K_B')$.

The proof of $K_G \cong K_G'$ is similar. □

With this lemma, we can proceed to draw and simplify RBG links associated to dualisable patterns and annulus twisting constructions.

Dualisable Patterns

We first observe the following restrictions for RBG links.

- $B \cup R \cong B \cup \mu_B, R \cup R \cong G \cup \mu_G.$

- The linking number between B and G is zero $lk(B, G) = 0$.

Note that this restriction is different from being a special RBG link. For simplicity, call this subset of RBG links the dualisable links.

We also note that for a dualisable link L, the two associated knots have diffeomorphic zero-traces. Indeed, we consider the RBG link as a Kirby diagram, with the R component as the 1-handle, and B, G component as 0-framed 2-handles. This yields a 4-manifold X. By sliding B over G, we can see that X is diffeomorphic to the zero-trace of the knot K_B. Similarly, X is also diffeomorhic to the zero trace of K_G. The two diffeomorphisms we denote Ψ_B and Ψ_G, and the combined trace diffeomorphism we denote Φ_L.

It turns out that the set of dualisable links is exactly the set of RBG links associated to the homeomorphism constructed from dualisable patterns [27] [37]. This is given by the following theorem in [37].

Theorem 2.13. *For any pair of knots K, K' arise from a dualisable link, there exists a dualisable pattern P such that $P(U) \cong K$ and $P^*(U) \cong K'$. Conversely, for any dualisable pattern P, there exists a dualisable link L such that the knots associated are $P(U)$ and $P^*(U)$.*

Proof. We only prove the first assertion with a constructive proof. Reversing the construction gives a proof for the second assertion.

We begin by isotoping the diagram such that R has no self-crossing and $B \cap D_R$ at a single point (D_R denotes the obvious disk R bounds in the diagram). From here we slide B under R such that B has no self crossings. We can do this since we can reverse any crossing by a single handle slide (c.f. Fig 5.11 of [15]). We record the signed number of slides required by s. Then we slide B across R ($-s$) times as indicated by the diagram below. We denote this link J_B and the diffeomorphism corresponding to the slides described above F_B.

13

Now we cut out the R component, and consider B and G as knots in $S^1 \times S^2$. Since both B and G are isotopic to $S^1 \times *$, we can consider $G \subset S^1 \times S^2 \nu(B) \cong S^1 \times D^2$ to be the pattern P.

By switching the role of B and G, we can accordingly define the link J_G, the diffeomorphism F_G, and the dual pattern P^*.

It is fairly easy to check that P and P^* defines a dualisable pattern. Also, it is immediate from the construction that the slam-dunk homeomorphism R and B in J composed with $F_B \circ \Psi_B^{-1}|_\partial$ defines a homeomorphism $S^3 \to S^3$ taking K_G to $P(U)$. Similarly we can prove that $K_B \cong P^*(U)$.

$\square$

From the above theorem and observations, we know that the dualisable patterns can be used to construct surgery homeomorphisms, and moreover the homeomorphism always extends to a zero-trace diffeomorphism.

Annulus Twisting

Finally we quickly explain how to draw RBG links associated to Annulus twistings. To do so, we directly follow the routine of Lemma 2.11 and get the leftmost picture of the following plot.
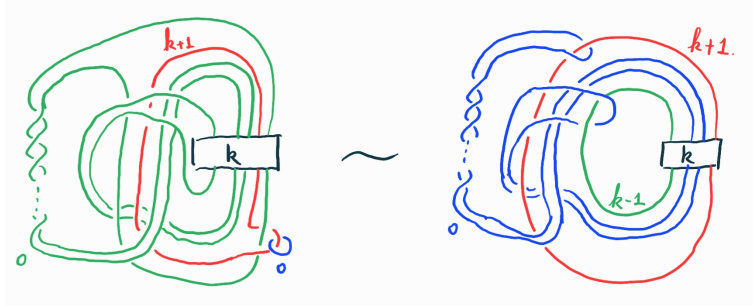
To make the RBG link easier to deal with, we make a few modifications. Sliding the G component over R gets us the middle picture. An isotopy gives the rightmost picture.

2.2 Equivalence Relations between Knot Traces

In this section, we will consider various equivalence relations in the study of 4-manifolds between knot traces . Also, since knot traces have non-trivial

boundary, we will also discuss the relative version of these equivalence relations, namely requiring the equivalence relation to respect the a priori fixed boundary diffeomorphism. We will give some detailed definitions below.
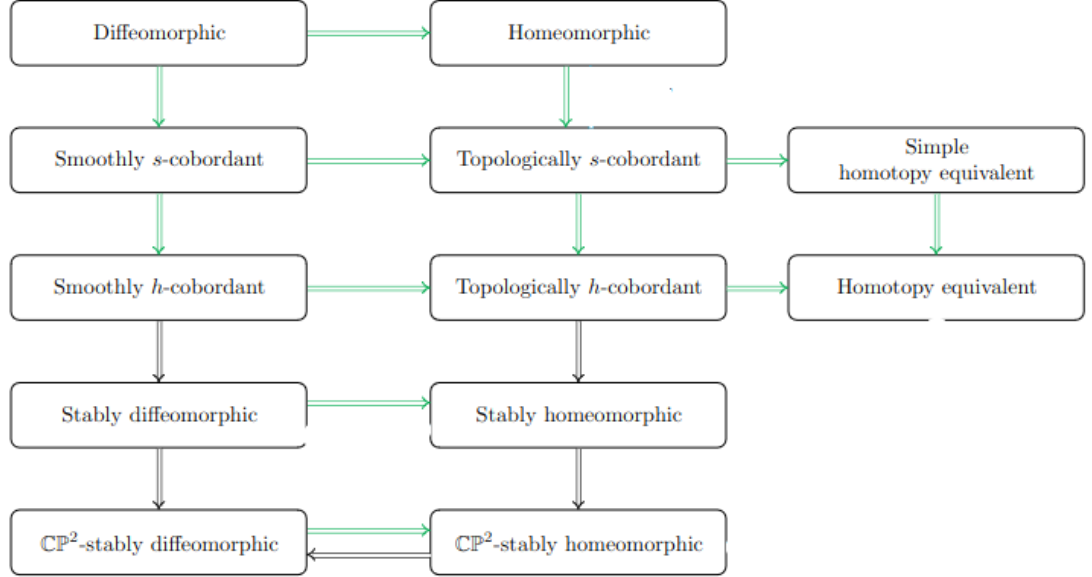
The equivalence relations considered in this section are depicted in the above chart [20]. However, since we are dealing with manifolds with nontrivial boundaries, for every equivalence relation in the chart there is a "relative" version and an "absolute" version.

Definition 2.14. Given two 4-manifolds X and Y with homeomorphic boundaries and a fixed boundary homeomorphism $f : \partial X \to \partial Y$, X and Y are said to be diffeomorphic (resp. homeomorphic, homotopy equivalent) relative to f, or relatively diffeomorphic (resp. homeomorphic, homotopy equivalent) for short, if the boundary homeomorphism f extends to a diffeomorphism (resp. homeomorphic, homotopy equivalent) $F : X \to Y$, i.e. $F|_{\partial X} = f$. If the choice of the boundary homeomorphism f is arbitrary, X and Y are said to be (absolutely) diffeomorphic (resp. homeomorphic, homotopy equivalent).

Note that a homotopy equivalence typically does not map a boundary to the boundary. Yet the above definition of relative homopy equivalence is still valid.

Definition 2.15. Given two 4-manifolds X and Y with homeomorphic boundaries and a fixed boundary homeomorphism $f : \partial X \to \partial Y$, X and Y are said to be h-cobordant (resp. s-cobordant) relative to f, or relatively h-cobordant (resp. s-cobordant) for short, if the closed 4-manifold $X \cup_f -Y$ bounds a 5-manifold with boundary W such that the inclusion maps $i_X : X \hookrightarrow W$ and $i_Y : Y \hookrightarrow W$ are homotopy equivalences (resp. simple homotpy equivalences). If the choice of the boundary homeomorphism f is arbitrary, X and Y are said to be (absolutely) h-cobordant (resp. s-cobordant).

Note that the above definition is valid both in the smooth category and the topological category. We will distinguish the resulting equivalence relations by smooth h-cobordisms (resp. s-cobordisms) and topological h-cobordisms (resp. s-cobordisms).

Definition 2.16. Given two 4-manifolds X and Y with homeomorphic boundaries and a fixed boundary homeomorphism $f : \partial X \to \partial Y$, X and Y are said to be relatively stably diffeomorphic (resp. homeomorphic) if there exists an integer $n \geq$ such that f extends to a diffeomorphism (resp. homeomorphism) $F : X \# n S^2 \times S^2 \to Y \# n S^2 \times S^2$. If the choice of the boundary homeomorphism f is arbitrary, X and Y are said to be (absolutely) stably diffeomorphic (resp. homeomorphic).

Definition 2.17. Given two 4-manifolds X and Y with homeomorphic boundaries and a fixed boundary homeomorphism $f : \partial X \to \partial Y$, X and Y are said to be relatively $\mathbb{CP}^2$-stably diffeomorphic (resp. homeomorphic) if there exist integers $m, n \geq$ such that f extends to a diffeomorphism (resp. homeomorphism) $F : X \# m \mathbb{CP}^2 \# n \overline{\mathbb{CP}^2} \to Y \# m \mathbb{CP}^2 \# n \overline{\mathbb{CP}^2}$. If the choice of the boundary homeomorphism f is arbitrary, X and Y are said to be (absolutely) $\mathbb{CP}^2$-stably diffeomorphic (resp. homeomorphic).

Note that most of the arrows in the chart of equivalence relations above are immediate. The fact that an h-cobordism implies stably isomorphic (in either categories) follows immediately from the proof of Wall's theorem [45]. The fact that stably isomorphic implies $\mathbb{CP}^2$-stably isomorphic follows from the diffeomorphism between $S^2 \times S^2 \# \mathbb{CP}^2 \cong \mathbb{CP}^2 \# \overline{\mathbb{CP}^2} \# \mathbb{CP}^2$.

Now we go back to knot traces. To start with, we know that since any two knots as maps $S^1 \to S^3$ are homotopic to each other, all 0-traces are homotopy equivalent to $X_0(U) \cong S^2 \times D^2 \simeq S^2$.

Also, since knot traces are simply connected, the whitehead torsion vanishes, and thus 0-traces are also simply homotpy equivalent to each other.

Similarly, two 0-traces are relatively (smooth) s-cobordant if and only if they are relatively (smooth) h-cobordant.

For more complicated equivalence relations, it can be summarised that the obstruction of two simply-connected 4-manifolds with boundary being homeomorphic rel boundary is Boyer's θ-obstruction [3], which is completely determined by the parity in the case of knot traces. This is completely understood. which will be discussed in detail in the first subsection. The obstructions of two knot traces being diffeomorphic is not yet completely understood. In the second subsection, we will discuss some known obstructions and counterexamples.

2.2.1 Topological Obstructions

All simplt-connected compact 4-manifolds with non-trivial boundary is classified by Boyer's result [3]. To start with, we quickly recall a version of Boyer's theorem.

Theorem 2.18. *Let X and Y are two 4-manifolds with homeomorphic boundary and equivalent Kirby-Siebenmann invariants and f be an orientation preserving homeomorphism on the boundaries. If there exists an isometry Λ between the intersection pairings of the two manifold such that the following diagram commutes*

$$
\begin{array}{ccccccccc}
0 & \longrightarrow & H_2(\partial X) & \longrightarrow & H_2(X) & \longrightarrow & H_2(X,\partial X) & \longrightarrow & H_1(\partial X) & \longrightarrow & 0 \\
 & & \downarrow{\scriptstyle f_*} & & \downarrow{\scriptstyle \Lambda_*} & & \uparrow{\scriptstyle \Lambda^*} & & \downarrow{\scriptstyle f_*} & & \\
0 & \longrightarrow & H_2(\partial Y) & \longrightarrow & H_2(Y) & \longrightarrow & H_2(Y,\partial Y) & \longrightarrow & H_1(\partial Y) & \longrightarrow & 0
\end{array}
$$

, then

- *If $H_1(\partial X;\mathbb{Q}) = 0$ or X is odd, then f always extends to a homeomorphism $F : X \to Y$.*

- *If $H_1(\partial X;\mathbb{Q}) \neq 0$ and X is even, then f extends to a homeomorphism $F : X \to Y$ if and only if the 4-manifold $X \cup_f -Y$ is spin.*

If we apply the above theorem of Boyer to the case of zero traces, stabilised zero traces, and $\mathbb{CP}^2$-stabilised zero traces, we have the following facts.

Lemma 2.19. *Given a pair of knots K and K' such that there is an orientation preserving homeomorphism $\phi : S_0^3(K) \to S_0^3(K')$. Then the following statements are equivalent*

1. *The boundary homeomorphism ϕ extends to a homeomorphism $\Phi : X_0(K) \to X_0(K')$.*

2. *The boundary homeomorphism ϕ extends to a homotopy equivalence $\Phi : X_0(K) \to X_0(K')$.*

3. *There is a relative h-cobordism between $X_0(K)$ and $X_0(K')$ corresponding to the map ϕ.*

4. *The boundary homoemorphism ϕ extends to a stable diffeomorphism $\Phi : X_0(K) \# n S^2 \times S^2 \to X_0(K') \# n S^2 \times S^2$.*

5. *The boundary homeomorphism ϕ extends to a stable homeomorphism $\Phi : X_0(K) \# n S^2 \times S^2 \to X_0(K') \# n S^2 \times S^2$.*

6. *The boundary homeomorphism ϕ is even, i.e. the 4-manifold $X(K) \cup_\phi -X(K')$ has even intersection form.*

Proof. $(5) \Rightarrow (6)$ and $(6) \Rightarrow (1)$ are direct applications of Boyer's theorem.

$(1) \Rightarrow (3)$ and $(3) \Rightarrow (4)$ are Wall's theorem: two homeomorphic simply-connected 4-manifolds are h-corbordant and thus stably diffeomorphic.

$(1) \Rightarrow (2)$ and $(4) \Rightarrow (5)$ are immediate.

For $(2) \Rightarrow (6)$, we prove by using a variation of Boyer's original proof. (The same idea can be used to prove $(5) \Rightarrow (6)$.)

By contradiction, assume that ϕ is odd.

Then we consider the following two closed 4-manifolds. Define $W := X_0(K) \cup_{id} -X_0(K)$ be the double of $X_0(K)$, which we know has even intersection form. Define $W := X_0(K) \cup_\phi -X_0(K')$ as usual, which has odd intersection form by assumption. We will build a homotopy equivalence $f : W \to X$, which leads to an immediate contradiction due to the difference of parity of the intersection forms.

Define $f : W \to X$ to be the identity on the first copy of $X(K)$, and the relative homotpy equivalence Φ on the second copy. Since Φ restricts to the homeomorphism ϕ on the boundary, we know that the map f is continuous.

Now we pick a tubular neighbourhood B for $S_0^3(K') \hookrightarrow X$. We pick a small enough tubular neighbourhood A for $S_0^3(K) \hookrightarrow W$ such that $f(A) \subset B$. With this condition, we can apply naturality of Mayer-Vietoris sequence. Up to homotpy equivalence, we have the following diagram.

$$0 \longrightarrow H_2(S_0^3(K)) \longrightarrow H_2(X_0(K)) \oplus H_2(X_0(K)) \longrightarrow H_2(W) \longrightarrow H_1(S_0^3(K)) \longrightarrow 0$$

$$0 \longrightarrow H_2(S_0^3(K')) \longrightarrow H_2(X_0(K)) \oplus H_2(X_0(K')) \longrightarrow H_2(X) \longrightarrow H_1(S_0^3(K')) \longrightarrow 0$$

Note that all verticals maps are induces by (the restrictions) of f, and all but the third one are isomorphisms. Thus $f_* : H_2(W) \to H_2(X)$ is also an isomorphism.

However, since W and X are constructed as simply connected manifolds, we combine the previous observsation with Hurewicz theorem and Whitehead theorem, we know that W and X are in fact homotopy equivalent, yielding the contradiction.

$\square$

Lemma 2.20. *Given a pair of knots K and K' such that there is an orientation preserving homeomorphism $\phi : S_0^3(K) \to S_0^3(K')$. Then ϕ always extends to a $\mathbb{CP}^2$-stable diffeomorphism between knot traces.*

Proof. By applying Boyer's theorem for odd 4-manifolds, we know that ϕ extends to a $\mathbb{CP}^2$ stable homeomorphism.

However, we can think of ϕ as a map $\partial(X(K)\#\mathbb{CP}^2) \to \partial(X(K')\#\mathbb{CP}^2)$. Wall's theorem told us that ϕ extends to a stable diffeomorphism for the blown-up knot traces and thus a $\mathbb{CP}^2$ stable diffeomorphism for the original knot traces. $\square$

Note that all of the above mentioned equivalence relations (except homotopy equivalence and simple homotopy equivalence) restrict to some boundary homeomorphism, thus we can also conlclude that two zero traces are (absolutely) homeomorphic if and only if they are stable homeomorphic if and only if they are s-cobordant.

Also note that we can easily apply Boyer's theorem to the case of $n \neq 0$ to study general knot surgery and traces. Since in this case the first homology of the n-surgery is pure torsion, the n-traces are always relatively homeomorphic (s-cobordant, ...) to each other.

Next we will introduce some concrete examples.

Gluck Twist

The first counterexample is given by Gluck [12], which shows that the above described topological obstruction could exist in the case of as easy as the unknot.

Consider $S_0^3(U) \cong S^2 \times S^1$ and the following map

$$\phi : S^2 \times S^1 \to S^2 \times S^1$$
$$(x, t) \mapsto (\Phi_t(x), t)$$

where Φ_t denotes the rotation along a fixed axis through an angle of $2\pi t$ if we consider S^1 as $\mathbb{R}/\mathbb{Z}$.

The map ϕ is odd, for if we glue two pieces of $X_0(U) \cong X_0(U)$ using this map, we will have $S^2 \tilde{\times} S^2$, as described by the following Kirby diagram on the right.

Note that to cut out an embedded copy of $S^2 \times D^2$ and glue it back in via the map ϕ gives the definition of the Gluck twist. The above two pictures describe the easiest Gluck twist, taking $S^2 \times S^2$ to $S^2 \tilde{\times} S^2$.

This examples shows that even in the simplest case, a 0-surgery homeomorphism might not extend to a 0-trace homeomorphism.

RBG Constructions

In the case of RBG constructions, we consider he following family of special RBG links called the Manolescu-Piccirillo family.
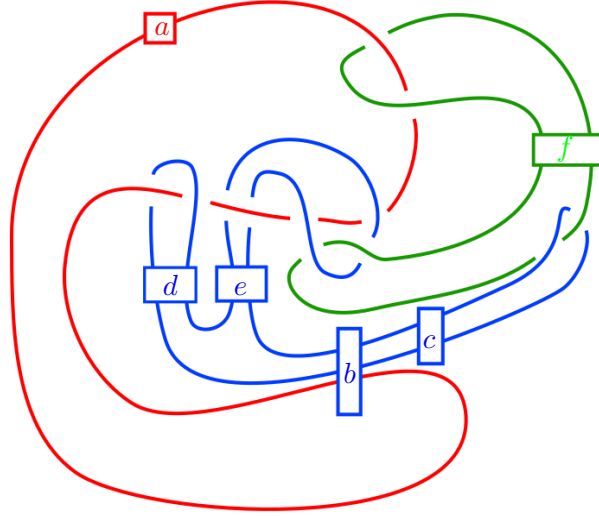
Figure 2.8: A family of examples of special RBG links

We will call an RBG link even (odd) if the associated homeomorphism $\phi_L : S_0^3(K_B) \to S_0^3(K_B)$ is even (odd), i.e. if and only if the 4-manifold $X_0(K_B) \cup_{\phi_L} -X_0(K_G)$ is even (odd).

Moreover, we have the following lemma.

Lemma 2.21. *A special RBG link is odd if and only is r is odd.*

Proof. Let $\gamma \subset S_0^3(K_B)$ be the framed image of the 0-framed meridian under the homeomorphism ϕ_L. By Akbulut's gluing upside-down trick, we know that $K_B \cup \gamma$ is a Kirby diagram for the manifold $X_0(K_B) \cup_{\phi_L} -X_0(K_G)$. Thus we know that the manifold is even if and only if the framing of γ is even, as we can reading off the intersection matrix from the Kirby diagram fairly easily.

21
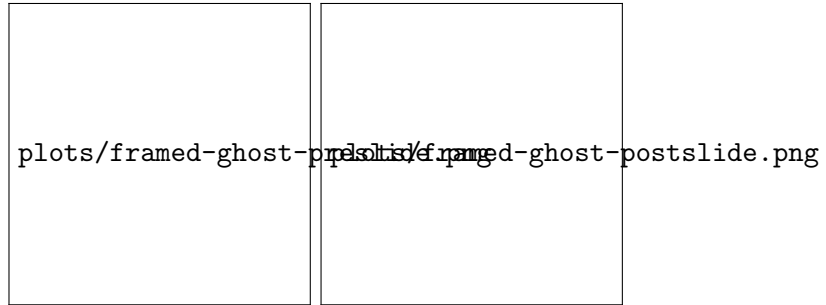
Now we show that γ is r-framed. Observe the first picture above of the local picture of the special RBG link. To get the knot K_B, we perform the slide indicated in the picture. As shown in the second picture, after the slides, γ can be considered as a framed ghost of R. In particular, γ is r framed.

$\square$

Combining the above results, we obtain the result that the boundary homeomorphism ϕ_L extends to a 0-trace homeomorphism if and only if r is even.

Annulus Twisting

In the case of Annulus twisting, we restrict our attetion to a specific family of knots. Denote the following family of knots by $J_m[k]$.
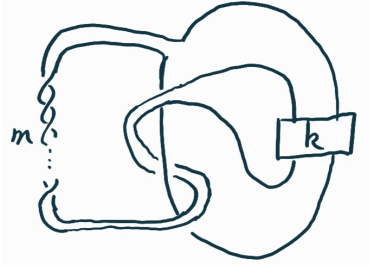
Note that the homeomorphism corresponding to annulus twisting once is even if and only if k is odd. This can be seen by keeping track of the meridian. Note that we can relate annulus twisting once of the above family of knots to the following (not necessarily special) RBG link.
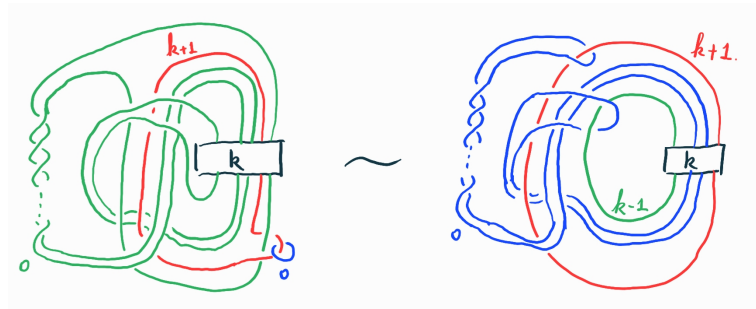
Dualisable Patterns

As we have discussed before, constructions via dualisable patterns described in the last section do not yield any counterexamples here. Moreover, the 0-traces constructed in this way are actually diffeomorphic to each other. Later, the notion of dualisable links will be generalised to what is called property U to construct pairs of diffeomorphic knot traces. This will be discussed more in detail in the following subsection.

Note that in the special case when the Mapping class group of the 0-surgery is trivial, the failure of boundary homeomorphism extending to the 0-trace actually means that the two knot traces are (absolutely) not homeomorphic.

By calculating the symmetry group with the help of Snappy [5], we found that even within the Manolescu-Piccirillo family, there exist RBG links that are odd such that $\mathcal{MCG}(S^3_{r,b,g}(R \cup B \cup G)) = 1$. The following diagrams describe such a pair of associated knots (in which case $(a, b, c, d, e, f) = (-2, 1, 2, 1, 2, 1)$ and thus $r = a + b = -1$). The detailed codes and results I used can be found at https://nickteng.github.io/pages/counterexamples.html.
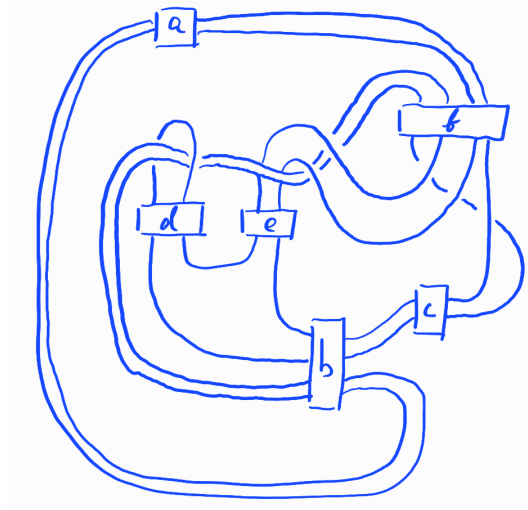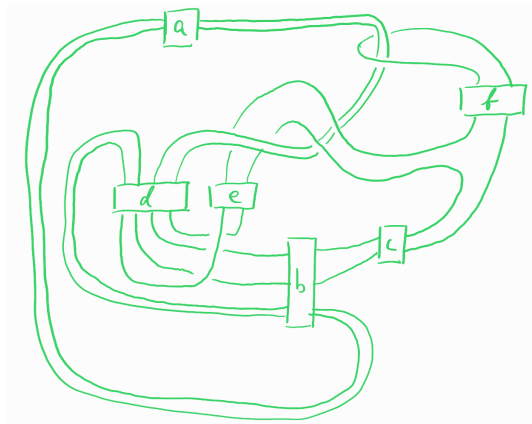
Note that this disproves the Freedman theorem in the case of nontrivial boundary.

2.2.2 Smooth Obstructions

On the matter of classifying knot traces up to diffeomorphism, things become more complicated. In fact, it is not yet completely understood whether or not the boundary homeomorphism extends to a trace diffeomorphism. However, we do have a sufficient condition called "property U" that ensures relative diffeomorphism. This property is closely related to (and in fact inspired by) the dualisable constructions, which will be the main focus in the first part of this section.

Turning to absolute exotica, although also not completely understood, we do have a few examples and ways of detection.

Generally speaking, almost all known smooth knot trace invariants are smooth knot concordance invariants. One such invariant is the ν invariant from Heegaard Floer theory, which is relatively easier to calculate thanks to the Heegaard Floer Calculator. This fact is given by the following theorem [16].

Theorem 2.22. *If the oriented knot traces $X_n(K)$ and $X_n(K')$ are diffeomorphic, then $\nu(K) = \nu(K')$, except possibly if $n < 0$ and $\{\nu(K), \nu(K')\} = \{0, 1\}$.*

This theorem provides us a tool for distinguishing the (absolute) diffeomorphism type for knot traces. For example, the associated 0-traces of the link $L(1, 1, 1, 1, 1, 1)$ in the MP family are homeomorphic (since in this case $r = 2$ is even), but has different ν-invariants: via the calculation of Snappy,

24

the ν invariant for the associated knot K_B vanishes while $|\nu(K_G)| = 2$. This gives us a first example for a pair of exotic knot traces. The proof of the above theorem, however, will be delayed to later sections of this survey.

As for examples of absolutely exotic knot traces, the first and most famous exotic pair is constructed by Yasui [46]. We will focus on the construction in the second part of this section.

Dualisable links and Property U

In the previous section, we have showed that all pairs of knots generated by dualisable patterns can be related by a dualisable link [37]. Thus knot traces generated by dualisable patterns are always relatively diffeomorphic. Later in [27], this was modified into a more general property called property U, defined as follows.

Definition 2.23 (Property U)**.** A 0-surgery homeomorphism $\phi : S_0^3(K) \to S_0^3(K')$ has property U if there is a diagrammatic choice of the framed knot $\gamma := \phi(\mu_K, 0)$ in the standard diagram of $S_0^3(K')$ such that γ is 0 framed and appears unknotted in the diagram.

Lemma 2.24. *A 0-surgery homeomorphism ϕ with property U extends to a 0-trace diffeomorphism.*

Proof. Following the schematic below, we give the following definitions. Let X be the tubular neighbourhood of the cocore of the 2-handle in $X_0(K)$. And let $X' \subset X$ be a open neighbourhood of the cocore, which is just a $D^2 \times \mathring{D}^2$. Let D be the standard slice disk of $\phi(\mu_K)$ in B^4 (the 0-handle of $X_0(K')$). Similarly define Y to be the tubular neighbourhood and D and Y' an open neighbourhood. Denote F' to be the natural bundle isomorphism $X \to Y$. Since both K and $\phi(\mu_K)$ are 0-framed, the isomorphism F' coincides with ϕ on the 0-surgery part of the boundary.

plots/schematic-X.png　plots/schematic-Y.png
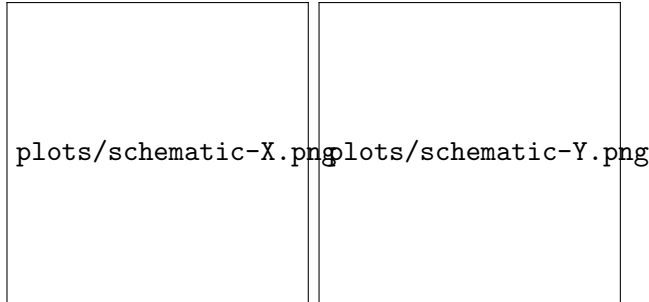
Note that the manifold $X_0(K)\backslash X'$ is clearly diffeomorphic to the standard B^4. We claim that the 4-manifold $X_0(K')\backslash Y'$ (clearly has boundary S^3) is diffeomorpphic to the standard B^4. Observe that $X_0(K')\backslash Y'$ has a Kirby diagram consisting of a 1-handle along $\phi(\mu_k)$ and a 0-framed 2-handle along K'. By surgering along the one handle, we can think of the boundary as S^3 obtained by surgery along a knot l in $S^1 \times S^2$. Gabai's proof of property R [11] ensures that l is isotopic to the standard $S^1 \times \{*\}$. Going back one step, we now know that the handles are actually a cancelling 1-2 pair. Thus the manifold $X_0(K')\backslash Y'$ is just diffeomorphic to the standard B^4.

Finally we construct the desired diffeomorphism. Note that we $F'|_{D^2 \times \partial D^2}$ and $\phi|_{\partial X_0(K)\backslash \nu_K}$ glues to a piecewise homeomorphism from $\partial(X_0(K)\backslash X')$ to $\partial(X_0(K')\backslash Y')$. However, this boundary homeomorphism extends to a diffeomorphism $F : X_0(K)\backslash X' \to X_0(K')\backslash Y'$ as there is only one isotopy class on S^3. Together with F', this defines a diffeomorphism between the knot traces.

□

The converse of the above lemma is still a conjecture.

One important application of the above observation is that if two knots K and K' are related to each other by an RBG link with property U, then K is slice if and only if K' is. [36] We will focus on this specific matter in later sections of this survey.

Yasui's Example

Finally we survey Yasui's construction [46]. This construction provides us an infinite family of examples of absolutely exotic 0-traces.

Consider the following patterns P_m and Q_m.
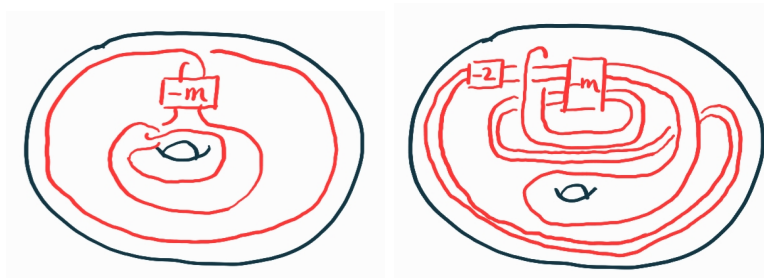
For simplicity, we fix $m = 0$. Note that the pattern P_0 is exactly the Mazur pattern.

Now consider the knot traces $X_0(P_0(K))$ and $X_0(Q_0(K))$ for some knot $K \subset S^3$. We claim that they are an (absolute) exotic pair.

We first prove that the two knot traces are homeomorphic. The knot traces are related by a cork twisting along an embedded Mazur cork. Indeed, this can be seen from the following picture: doing a zero-dot surgery on the Mazur cork in the leftmost picture $(X_0(P_0(K)))$ yields the middle picture, which is isotopic to the rightmost picture $X_0(Q_0(K))$.

However, this operation does not change the homeomorphism type by the following theorem of Freedman [9].

Theorem 2.25. *Any homoemorphism on the boundary of a contractible 4-manifold extends to a homeomorphism of the 4-manifold.*

Thus we have shown homeomorphism between the two knot traces.

Next we prove non-diffeomorphism. Now we require the knot K to satisfy $2g_4(K) = \overline{ad}(K) + 2$ and $\widehat{tb}(K) \geq 0$, where

- $\overline{ad}(K)$ denotes the maximal adjunction number among all Legendrian representatives for the knot K,

27

- $\widehat{tb}(K)$ denotes the maximal Thurston-Bennequin number among all Legendrian representatives $\mathcal{K}$ for K satisfying $ad(\mathcal{K}) = \overline{ad}(K)$.

Note that under this requirement, we can add zig-zags to find a Legendrian representative $\mathcal{K}$ for K such that $ad(\mathcal{K}) = \overline{ad}(K)$ and $tb(\mathcal{K}) = 0$. A first example for this requirement is just the right-handed trefoil knot $T_{2,3}$. Now we can find a Legendrian representative for the knot $P_0(K)$ and $Q_0(K)$. These are captured by the following pictures.

From the pictures, we can read off that for the Legendrian representative for $P_0(K)$ described above, it has $tb = tb(\mathcal{K})$ and rotation number $|r| = |r(\mathcal{K})|$. By adding a zig-zag to the picture above, we get a Legendrian representative with $tb = 1$ and $|r| = |r(\mathcal{K})| + 1$.

Now, to show that the knot traces are not diffeomorphic, we compare their 0-shake genera. To do so, we need the following facts.

- By applying the Stein adjunction inequality [22], we have $|r(K)| + 1 \leq 2g_s^{(0)}(P_0(K)) - 2$. This implies $g_s^{(0)}(P_0(K)) \geq \frac{1}{2}(|r(K)| + 3) = \frac{1}{2}(\overline{ad}(K) + 4) = g_4(K) + 1$.

- The knots K and $Q(K)$ are concordant. Thus they have the same slice genus.

- The slice genus of any knot is larger or equal to its 0-shake genus.

Combining the above three results, we have the inequality $g_s^{(0)}(P_0(K)) \geq g_4(K) + 1 > g_4(Q_m(K)) \geq g_s^{(0)}(Q_0(K))$. Thus the two knot traces are not diffeomorphic.

Note that the above construction can be easily generalised to any n-trace. For details, see [46].

2.3 Knot Traces as Plugs

In [1], Akubulut and Yasui first define the term "plugs". A plug is a Stein manifold that acts like the non-simply-connected analogy for corks. For simplicity, we remove the Stein condition on the manifold and the involution condition on the foundary map, calling it a (loose) plug. To be precise, we give the following definition.

Definition 2.26. A (loose) plug is a pair (W, f) such that W is a compact 4-manifold with non-trivial boundary, and $f : \partial W \to \partial W$ a diffeomorphism of 3-manifolds satisfying:

- f does not extend to an automorphism (in either TOP or SMooth category) of W.

- W embeds in some 4-manifold X such that $X \backslash W \cup_f W$ provides an exotic copy of X.

Just like the cork case, we call the operation $X \mapsto X \backslash W \cup_f W$ a plug twist.

In this section, we focus on knot traces acting as plugs. In the first subsection, we will see that by plug twisting zero traces for topologically slice but not smoothly slice knots, we get exotic $\mathbb{R}^4$s. In the second subsection, we will modify the technique a little bit and survey some results on attempting to find exotic S^4s. In the last subsection, we prove that there exist knot traces acting as infinite order plugs (just like its cork counterpart in [14]).

2.3.1 Exotic $\mathbb{R}^4$'s

In this section we relate the plug twisting problem for zero traces to sliceness problems and construct am infinite family of exotic $\mathbb{R}^4$s. We start with the essential tool to study knot traces as plugs: the trace embedding lemma, stated as follows.

Theorem 2.27. *For a knot K, K is slice if and only if its $X_0(K)$ embeds in S^4.*

Proof. We first prove the "only if direction". S^3 decomposes S^4 into two pieces. We put out knot K in S^3 and consider one of the two pieces as the 0-handle. Since K bounds a disk in the other piece, we can take its tubular neighbourhood and consider it as the 2-handle. Togeter we have constructed an embedded 0-trace.

Now we prove the "if" direction. Consider the piecewise linear embedding $F : S^2 \to X^4$ whose image consists of the core of the 2-handle and a cone over the knot K. Composing with the assumed embedding, we get a piecewise linear embedding $\iota \circ F : S^2 \to S^4$. Cutting out a small neighbourhood of the cone point, we get a "nice" embedding $D^2 \to D^4$, whose boundary of the image is the knot K. Thus the image defines the slice disk that we seek. The idea of the proof is given by the following picture.

$\square$
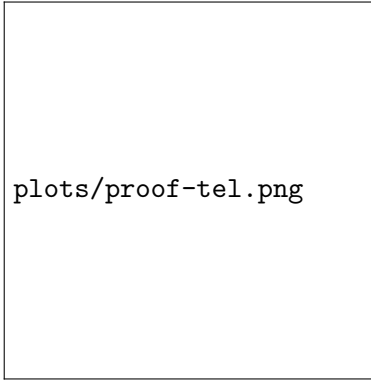
Note that the theorem and the proof work in both the TOP category and the Smooth category. Also note that in the statement of the theorem, it doesn't matter whether we choose to use the space S^4 or $\mathbb{R}^4$, or B^4.

Remark. There are several generalisations for the trace embedding lemma.

1. The ambient space can be changed from B^4 to any closed 4-manifold W. In this settings, the trace embedding lemma generalise to:

   Lemma 2.28. *A knot $K \subset W \backslash B^4$ is H-slice (that is, bounds a null-homologous disk) if and only if $-X_0(K)$ embeds in W by an embedding that induces the zero map on second homology.*

2. If we push off the slice disk D in $W \backslash B^4$, we can define an integral framing on K. In this settings, the trace embedding lemma generalise to:

   Lemma 2.29. *A framed knot (K, k) in $W \backslash B^4$ is slice (that is, bounds a framing-k disk) if and only if $-X_k(K)$ embeds in W.*

   For more details, see [29].

3. In [18], Hayden and Piccirillo generised the notion of knot traces to what is called "n-framed, genus g traces $X_n^g(K)$", that is, B^4 with a "thickened" punctured genus g surface glued along the knot K. Under this settings, the generalised trace embedding lemma becomes:

   Lemma 2.30. *For a knot $K \subset W \backslash B^4$, $-X_n^g(K)$ embeds into W if and only if the mirror $-K$ bounds a smooth genus g surface Σ in $W \backslash B^4$ with $[\Sigma] = \beta \in H_2(W \backslash B^4, S^3) \cong H_2(W)$ such that $\beta \cdot \beta = n$, where β is the image of the generator of the second homology of $X_n^g(K)$ under the map induced by the embedding.*

Now if we have a knot K that is topologically slice but not smoothly slice, we know immediately from the trace embedding lemma that its zero-trace $X_0(K)$ admits a locally flat embedding into $\mathbb{R}^4$, but there is no smooth embedding.

Removing the knot trace via the locally flat embedding yields a topological 4-manifold $U := \overline{\mathbb{R}^4 \backslash X_0(K)}$. It turns out that this manifold admits a smooth structure, as do all non-compact, connected, 4-manifolds. This result is given by the following theorem [39], [23], [7] [40].

Theorem 2.31. *The natural map $TOP(4)/O(4) \to TOP/O$ is 5-connected. In particular, every non-compact, connected component of a topological 4-manifold admits a smooth structure.*

Proof. Proof omitted as it's way beyond the scope of this survey. For details, see e.g. Chapter 21 of [2]. $\square$

Next we glue U and $X_0(K)$ back together. We can do this since every homeomorphism of a 3-manifold is isotopic to a diffeomorphism. This gives us a new smooth 4-manifold $\mathcal{R}$.

Tautologically $\mathcal{R}$ is homeomorphic to $\mathbb{R}^4$. However, we know that $X_0(K)$ embeds smoothly into $\mathcal{R}$. Thus $\mathcal{R}$ cannot be diffeomorphic to the standard $\mathbb{R}^4$ by the trace embedding lemma.

Finally we give some explicit examples. The most famous knot that is topologically slice but not smoothly slice is the Conway knot 11n34. This knot has trivial Alexander polynomial, and thus is topologically slice [7]. As for non-sliceness, the problem remained a conjecture for decades until finally solve by Piccirillo [36]. More details will be shed in the next chapter.

2.3.2 Attempt on Exotic S^4's

One of the most famous conjecture and motivating question in 4-manifold topology is the smooth 4 dimensional Poincaré conjecture (SPC4).

Conjecture. Every homotopy 4-sphere is diffeomorphic to the standard 4-sphere.

A naive attempt to find a counterexample for SPC4 (i.e. an exotic 4-sphere) is to directly apply the same technique used in the last subsection. However, the carved out topological manifold $S^4 \backslash X_0(K)$ is no longer non-compact, and does not necessarily have a smooth structure. Thus we need some modification to attempt on disproving SPC4.

In [27], Manolescu and Piccirillo proposed an attempt on constructing exotic S^4's. The same attempt can also be applied to detect exotic $\#^n \mathbb{CP}^2$'s. By convention, $\#^0 \mathbb{CP}^2$ denotes the 4-sphere. In what follows, let W denote a standard $\#^n \mathbb{CP}^2$.

Manolescu-Piccirillo ask the following question: does there exist pairs of knots (K, K') in $W^\circ := W \backslash B^4$ satisfying the following properties:

1. There exists a 0-surgery homeomorphism $\phi : S^3_0(K) \to S^3_0(K)$.

2. K is H-slice in W.

3. K' is not H-slice in W.

If the answer to the question above is positive, then we can construct an exotic copy of W. Indeed, by cutting out a copy of the zero-trace $X_0(K)$ (applying the trace embedding lemma) and plugging in $X_0(K')$, we have a closed

manifold X homeomorphic to the original manifold W. Here the homeomorphism is ensured by the Freedman classification, as the knot trace surgery leaves the homology of the 4-manifold unchanged. On the other hand, since the newly constructed manifold X has a zero-trace of K' smoothly embedded inside, we know that K' has to be H-slice in X. Combining with the third property above, we know that X cannot be diffeomorphic to W.

Unfortunately, the question posed above remains open and there remains no example of a pairs of knot satisfying the above three conditions. Consequently, we take one step back and find promising possibilities instead. To be specific, we nullify the second restriction above and transfer the exotica problem to a sliceness problem.

Recall from the first section that every 0-surgery can be represented by a RBG link. Also recall that for a knot K to be H-slice in some $\#^n \mathbb{CP}^2$, its Rasmussens's invariant $s(K)$ has to be non-negative [25]. Under this settings, we transfer our problem into finding RBG links L with associated knots K and K' such that:

1. The sliceness of K is not determined. In particular, its s-invariant vanishes $s(K) = 0$.

2. The s-invariant for K' is negative. In particular, K' is not H-slice in any $\#^n \mathbb{CP}^2$.

To find interesting examples of RBG links, Manolescu and Piccirillo went through 3375 links in the Manolescu-Piccirillo family of RBG links (Fig 2.8), with $a, c, e \in [-2, 2], b, d, e \in [-1, 1]$, and found 23 promising examples. Among the 23 knots, five knots have vanishing Alexander polynomial and thus are topologically slice [9]. The five knots (picture below) were candidates for being slice, and thus candidates for exotic 4-spheres. The rest of the 18 knots were proved to be algebraic but not topologically slice, and thus are only candidates for exotic $\#^n \mathbb{CP}^2$'s. We leave the details to [27].
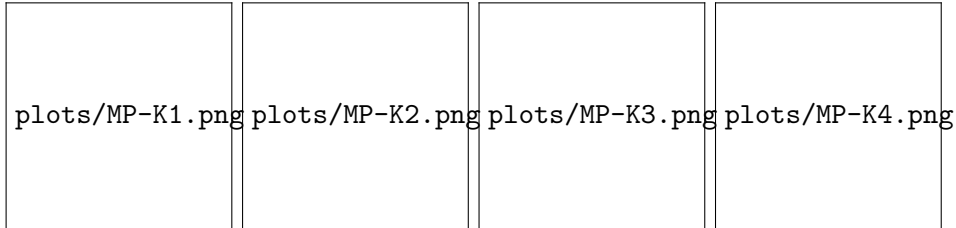
Unfortunately, in 2022 Nakamura proved in [29] that the five knots above are in fact not slice. To be precise, he proved the following:

Lemma 2.32. *Let (L, K, K') be a special RBG link and its associated knots satifying the following conditions:*

- *The red component R is the unknot U.*

- *B bounds a properly embedded disk Δ_B intersecting R in 1 point, and intersecting G in at most 2 points.*

- *G bounds a properly embedded disk Δ_G intersecting R in 1 point, and intersecting B in at most 2 points.*

(Note that the last two conditions are called the small RBG conditions in [27] and [29].)

Then we have the followings

- *If K is H-slice in some $\#^n\mathbb{CP}^2$, then $s(K') \geq 0$.*

- *If K is H-slice in some $\#^n\overline{\mathbb{CP}^2}$, then $s(K') \leq 0$.*

- *If K is slice in S^4, then $s(K') = 0$.*

Proof. See [29]. $\square$

In particular, this applies to all of the Manolescu-Piccirillo family of RBG links. Consequently, the five "promising" knots are not slice, and all 23 knots are not candidates for exotic $\#^n\mathbb{CP}^2$.

It is worth noting that Nakamura's results does not close the door for finding exotic S^4's and $\#^n\mathbb{CP}^2$'s in the technique introduced by Manolescu-Piccirillo. In particular, the Manolescu-Piccirillo family of RBG links can still possibly yield interesting examples, given that we do not obstruct sliceness by the Rasmussen's s-invariant. Also, if we fix on using the s-invariant, general RBG-links can still provide interesting examples.

Most recently in 2023, Qianhe Qin generalised the construction of RBG links to represent dehn-surgeries of all integral slopes [38]. Also, machine learning is used to detect ribbon knots [10]. Both results might shed some light on the constructions of new exotic manifolds.

2.3.3 Infinite Order Plugs

In 2017, Robert Gompf proved the existence of infinite order corks [14]. Namely, there exists a cork (C, f) such that f^k does not extend to a self-diffeomorphism of the cork for any k. In fact, if we do a cork twist via such maps f^k, it is possible to result in pairwise non-diffeomorphic 4-manifolds. In this section, we will adopt this idea to show that knot traces can actually behave as infinite order plugs. This is given by the following theorem.

Theorem 2.33. *There exists a knot trace $X_n(K)$ and a boundary automorphism ϕ on $S_n^3(K)$ such that the iterated automorphism ϕ^k does not extend to a trace automorphism for any $k > 0$.*

Note that if a boundary homeomorphism f actually extends to the knot trace, a plug twist will not change the diffeomorphism type of a 4-manifold. Thus to prove this theorem, we wish to find a (closed) 4-manifold containing $X_n(K)$ such that doing a plug twist via ϕ^k with result in pairwise non-diffeomorphic 4-manifolds.

To do so, we will take the closed 4-manifold to be the elliptic surface $E(m)$. We know from Fintushel and Stern's work that if $n \geq 2$, the knot surgery construction of $E(m)$ using a collection of knots distinguished by Alexander polynomials can result in a collection of pairwise exotic 4-manifolds [8]. Here we take the collection of knots to be the twist knots K_k, described by the following diagram.
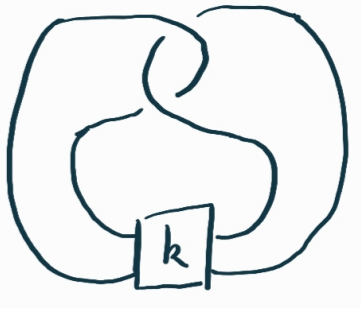
Thus to prove theorem 2.33, we only need to prove the following lemma.

Lemma 2.34. *There exists a knot trace $X_n(K)$ and a boundary automorphism ϕ such that $X_n(K)$ embeds in $E(m)$, and twisting this knot trace via the boundary automorphism ϕ^k will change the diffeomorphism type of $E(m)$ to the knot surgered 4-manifold $E(m)_{K_k}$ for any $k \geq 0$.*

Now observe the following picture of $M_0 := S^3 \backslash K_0$ near the top clasp.
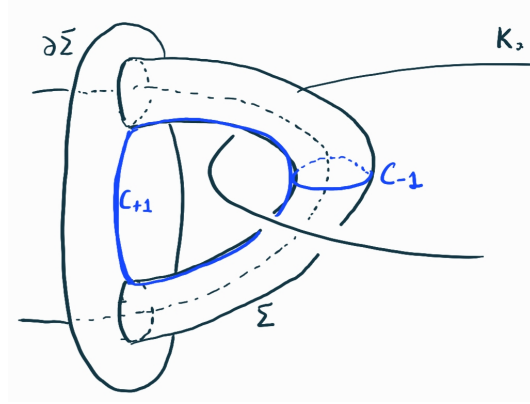
Let Σ be the punctured torus depicted in the picture. Note that we can get $M_k := S^3 \backslash K_k$ by simply doing a $-(\frac{1}{k})$-Dehn surgery on $\partial \Sigma$. This means we can get M_k from M_0 by slitting M_0 open along $I \times \partial \Sigma$ and reglue by g^k for some Dehn twist g, and get $E(m)_{K_k}$ from $E(m) = E(m)_{K_0}$ by slitting $E(m)$ open along $N := I \times \partial \Sigma \times S^1$ and reglue by $g^k \times id_{S^1}$.

Now if the boundary of a knot trace in $E(m)$ contains the manifold N, we can build a boundary homeomorphism by extending $g \times id_S^1$ as identity over the rest of the boundary. A plug twist with this boundary homeomorphism will solve the previous lemma. Thus we can update our goal to this following lemma.

Lemma 2.35. *There exists a knot trace $X_n(K)$ embedded in $E(m)$ whose bondary contains the 3-manifold N.*

Proof. Note that throughoout this proof, $I = [-1, 1]$.

We start with the manifold $Y := I \times \Sigma \times S^1 \subset E(m)$, whose boundary clearly contains N but is not simply connected. Its fundamental group has three generators: the two generators $C^*_{\pm 1} := \{\pm 1\} \times C_{\pm 1} \times \{*\}$ coming from M_0, and a third generator $\gamma_{-1} := \{-1\} \times \{*\} \times S^1$ coming from the S^1 factor in the multiplication. Attach a (-1)-framed 2 handle along each of the three generators gives a new 4-manifold Y' that is simply connected. Moreover, since we are attaching handles on the $\partial I \times \Sigma \times S^1$ part of the

boundary, N is still contained in the boundary of Y'. Also note that in the definition of knot surgery, the meridians of the knot K_k and the S^1 factor in the multiplication are identified to a near-cusp regular fibre of the elliptic fibration, and thus have $6m$ parallel copies of vanishing cycles. Thus in the above modification of Y, the three (-1)-framed 2-handles matches the vanishing cycles of $E(m)$ and thus Y' actually embeds in $E(m)_{K_0} = E(m)$.

Now the manifold Y' has two generators for the second homology: the tori $T_{\pm 1} := \{0\} \times C_{\pm 1} \times S^1$. We wish to kill the two generators and attach a new 2-handle to get the correct homotopy type.

To do so, we cap off the annuli $I \times C_{\pm 1}$ with the core of 2-handles attached before, and drill out small tubular neighbourhoods of the two disks $D_{\pm 1}$. Note that this new 4-manifold is still simply connected, since $T_{\pm 1}$ together with the core of the 2-handle attached along γ_{-1} can be seen as an immersed sphere, which acts as a null-homotopy of the meridian of the disks $D_{\pm 1}$. The 4-manifold also has no second homology by a quick Mayer-Vietoris sequence statement. In fact, this contractible manifold is Gompf's first example of an infinite order cork.

Lastly, to get the correct homotopy type, we add one more (-1)-framed 2-handle along the curve $\gamma_{+1} := \{+1\} \times \{*\} \times S^1$. For a similar reason in the last paragrapgh, the resulting 4-manifold X still embeds in $E(m)$ since γ_{+1} matches another vanishing cycle, and contains N in its boundary.

Finally we show that this 4-manifold X is indeed diffeomorphic to a knot trace. To do so, we will draw out the kirby diagram of each step in the construction.

We start with the 0-framed Borromean ring, which is the surgery diagram for the 3-torus $\mathbb{T}^3$. Changing one of its framing to $*$ (which means knot complement) will change this 3-manifold to $Q := \Sigma \times S^1$. Our manifold Y is just $I \times Q$.

Next we notice that adding a 2-handle to $I \times Q$ along some sphere $S \subset \{1\} \times Q$ and drilling out its core extended to $\{-1\} \times Q$ result in the 4-manifold $I \times P$, where P is the Dehn Surgery of Q along S. Using this observation, we now know that our manifold X is $I \times P$ with two additional (-1)-framed 2-handles, where P is described by the surgery diagram in figure 2.9.
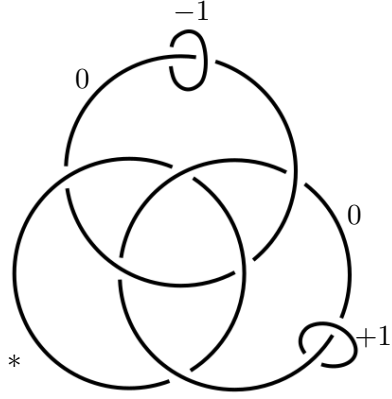
Figure 2.9: A surgery diagram of the 3-manifold P

Notice that in the picture above, the two framings of the surgery circles are ± 1-framed instead of (-1)-framed. This is because the circles $C_{\pm 1}$ lives on opposite faces of Y and thus inherit opposite orientations. Now after several Rolfsen twists, we have the surgery diagram described by the first picture below. Applying Akbulut's technique of drawing Kirby diagrams of knot complements, we know that the second picture below gives a Kirby diagram for the manifold $I \times P$.
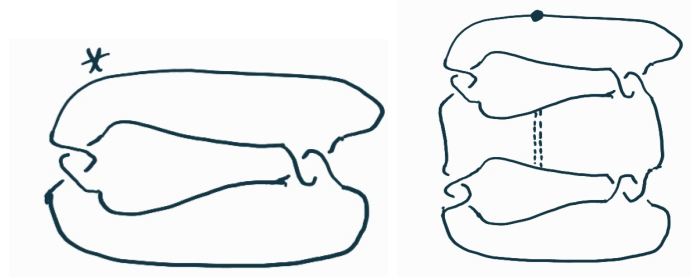
Finally we recover the normal 1-handle notation from the ribbon complement notation, and attach the last two 2-handles. This gives a description of our 4-manifold X, by the first Kirby diagram below. Cancelling the -1-framed 2-handles with the corresponding 1-handles, we clearly have a knot trace, which is described by the Kirby diagram on the right.

$\square$
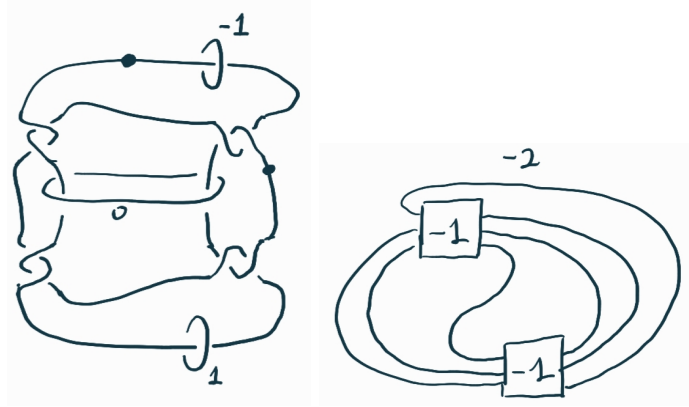
This finishes the proof of Theorem 2.33.

Note that a similar result in the topological category cannot hold. This is ensured by the following (stronger) result of Boyer.

Theorem 2.36. *For a compact simply-connected 4-manifold V with connected boundary M, there is an integer n depending only on $H_1(M)$ such that for any orientation preserving boundary automorphism f, f^n extends to a self-homeomorphism of V.*

Chapter 3

Knot Traces and Concordance Invariants

3.1 Khovanov Theory

In late 1990s, Mikhail Khovanov introduced a knot and link invariant called the Khovanov homology [19]. Later, Eun Soo Lee refined the Khovanov homology to a spectral sequence whose E_2 page recovers the original Khovanov homology [21]. In 2004, Jacob Rasmussen used the spectral sequence to define a knot concordance invariant $s(K)$ [42]. Additionally, Rasmussens shows that the s-invariant is in fact a lower bound for the slice genus.

In [36], Lisa Piccirillo applied techniques from dualisable patterns to construct a pair of knots with diffeomorphic knot traces but distinct Rasmussen's s-invariants. Additionally, she showed that neither the s-invaiant nor the slice genus is a knot trace invariant. Later in [37], she applied this fact to prove that the Conway knot is not slice. We survey her results in the next section. In this section, we follow the routine of [42] to recall some related constructions in Khovanov theory.

3.1.1 The Cube of Resolutions

Both Khovanov homology and Lee's modified homology can be constructed via some $1 + 1$-dimensional TQFT to what is called a cube of resolutions.

To start with, we construct a cube of resolutions. If we are given a link diagram L with k crossings, ordered from 1 to k, the associated cube of resolutions is a k-dimensional cube equipped with the following data:

- For each vertex $v = (v_1, ..., v_k)$ of the cube, we associate a 1-manifold

Figure 3.1: 0- and 1- resolutions of a crossing

D_v, where D_v is represented by the link diagram where the ith crossing is resolved in the way indicated by the number $v_i \in \{0, 1\}$, as indicated by the figure below. Note that since all crossings are resolved in some way, D_v is just an unlink.

- For each edge e connecting vertices $v_e(0)$ and $v_e(1)$, the diagrams for $D_{v_e(0)}$ and $D_{v_e(1)}$ differ only near a single crossing. Thus we can associate the edge e with a $1+1$ dimensional cobordism $S_e : D_{v_e(0)} \to D_{v_e(1)}$ where S_e is the saddle cobordism near the targeted crossing and the trivial cobordism anywhere else.

The following picture gives an example of a cube of resolutions for the trefoil.

Now if we have a $1+1$-dimensional TQFT $\mathcal{A}$, we can define a cohomology theory as follows:

- The underlying group in the complex is defined to be $\bigoplus_v \mathcal{A}(D_v)$.

- The differential is defined as follows: given an element $x \in \mathcal{A}(D_v)$, its differential is the sum of the TQFT evaluated on edges with x acting as the initial end. To be rigorous, denote $c_0(v)$ as the number of crossings with a type 0 resolution, and e_i some edge representing a resolution change, then we can define

$$d = \sum_{i=1}^{c_0(v)} (-1)_i^s \mathcal{A}(S_{e_i})$$

, where s_i are some choice to ensure $d \circ d = 0$. Note that different choices of s_i all yield isomorphic chain complexes.

- The homological grading is defined by $gr(v) := |v| - n_-$, where $|v|$ is the number of 1's in its coordinates, and n_- is the number of negative crossings in the original link diagram.

41
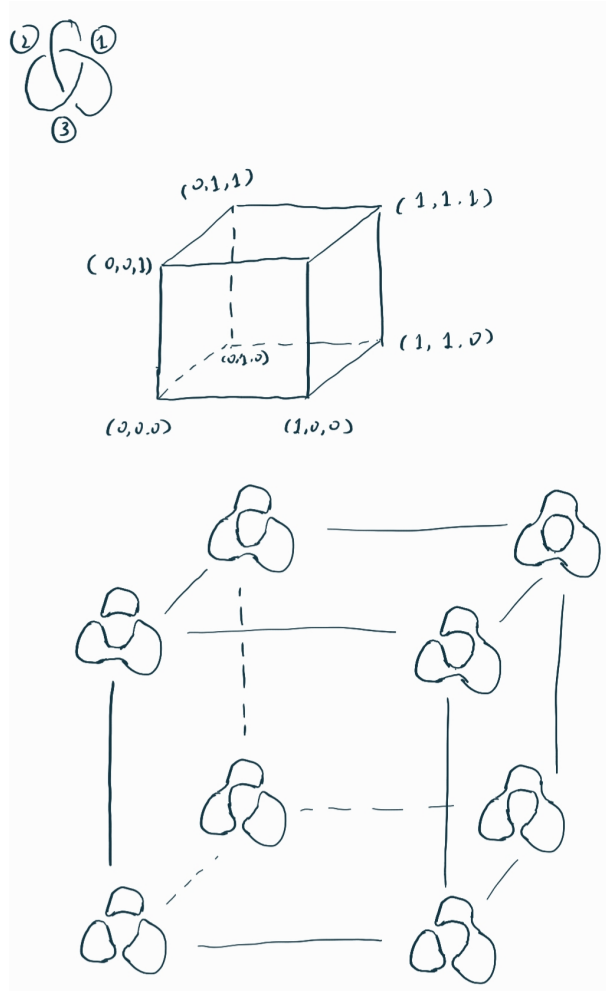
Figure 3.2: The cube of resolutions for a trefoil.

42

Since the differential increases the homological grading by 1, we yield cohomology theories if we have a reasonable choice for the TQFT $\mathcal{A}$. In the next two parts of this section, we will define Khovanov's TQFT and Lee's TQFT to yield Khovanov homology Kh and Lee's modified Khovanov homology Kh'.

3.1.2 Khovanov Homology

To define Khovanov's TQFT $\mathcal{A}$, we start by describing the action of $\mathcal{A}$ on vertices of the cube of resolutions. Let V be a vector space spanned by two elements v_+ and v_-. We define $\mathcal{A}(D_v) := V^{\otimes n}$, where n is the number of disjoint circles in the diagram associated to D_v.

Next we specify how $\mathcal{A}$ acts on morphisms. Recall that for each edge e in a cube of resolutions, the two diagrams associated to the vertices connected are exactly the same except near a crossing. This tells us that the cobordism associated to the edge is the trivial cobordism for circles away from the crossing, and is a pair of pants near the crossing. Thus, $\mathcal{A}(S_e)$ is given by one of the two following maps:

- $m : V^{\otimes 2} \to V$, which is associated to the cobordism of merging two circles into one. The specific formula is given by $m(v_+ \otimes v_+) = v_+$, $m(v_+ \otimes v_-) = m(v_- \otimes v_+) = v_-$, and $m(v_- \otimes v_-) = 0$.

- $\Delta : V \to V^{\otimes 2}$, which is associated to the cobordism of splitting a circle into two. The specific formula is given by $\Delta(v_+) = v_+ \otimes v_- + v_- \otimes v_+$ and $\Delta(v_-) = v_- \otimes v_-$.

With the TQFT $\mathcal{A}$ defined above, we have the Khovanov cochain complex $CKh(L)$. Again note that the differential d increases the homological grading gr by 1.

Finally we define another grading q for Khovanov homology, also known as the quantum grading (or q-grading for short). To start with, we first define a grading p for the TQFT by setting $p(v_\pm) = \pm 1$, and extend it to all of $V^{\otimes n}$ by $p(v_1 \otimes ... \otimes v_n) = p(v_1) + ... + p(v_n)$. Note that we have $p(S_e(v)) = p(v) - 1$ if $v \in V^{\otimes n}$ is a homogeneous element. Then we can define the quantum grading q on Khovanov chain complex CKh by $q(v) := p(v) + gr(v) + n_+ - n_-$, where $n_\pm$ denotes the number of positive and negative crossings in the initial diagram L. With this definition, we can see that $q(d(v)) = q(v)$, i.e. the differential preserves the quantum grading.

Remark. Note that the existence of $n_\pm$ in the definition of the quantum grading is to ensure that the grading is invariant under different choices of the link diagram L.

Remark. Note that the graded (with respect to q) Euler characteristic is the normalised Jones polynomial of L.

Thus we know that the Khovanov complex splits into direct sum of complexes for each quantum grading. The cohomology of $CKh(L)$ (thought as a bigraded group) is the Khovanov homology $Kh(L)$.

3.1.3 Lee's Modified Khovanov Homology

Next we construct Lee's modified Khovanov homology $\mathcal{A}'$. To do so, we only need to modify the TQFT a little bit.

- The underlying group of the cochain complex is exactly the same as the case of the original Khovanov homology, i.e. $\mathcal{A}'(D_v) = \mathcal{A}(D_v) = V^{\otimes n}$.

- The action of $\mathcal{A}'$ on morphisms is given by the following two modified maps $m' : V \otimes V \to V$ and $\Delta' : V \to V \otimes V$, where

$$m'(v_+ \otimes v_+) = m'(v_- \otimes v_-) = v_+ \qquad m'(v_+ \otimes v_-) = m'(v_- \otimes v_+) = v_-$$
$$\Delta'(v_+) = v_+ \otimes v_- + v_- \otimes v_+ \qquad \Delta'(v_-) = v_+ \otimes v_+ + v_- \otimes v_-.$$

The constructed cochain complex is Lee's modified Khovanov complex $CKh'(L)$, and the associated cohomology theory is Lee's modified Khovanov homology $Kh'(L)$.

Remark. Since Lee's modilied Khovanov complex has the exact same underlying group as the original Khovanov complex, we can define the quantum grading q accordingly. Although q does not behave quite so well as in the original Khovanov homology, it defines a filtration on $CHk'(L)$, and leads to the following theorem proved in [21].

Theorem 3.1. *There is a spectral sequence converging to $Kh'(L)$ whose E_2 page recovers the Khovanov homology $Kh(L)$. Moreover, every E_n page is a link invariant $\forall n \geq 2$.*

We finish this subsection by very briefly introducing the behaviour of Kh' under cobordism of knots, since this plays an important role in the understanding of the Rasmussen's s- invariant. Of course there is also a

Figure 3.3: Reidemeister moves and Morse moves.

similar definition for the original Khovanov homology, but it is out of the scop of this survey.

Given a cobordism S bewteen two links L and L', we wish to construct an induced map $\phi_S : Kh'(L) \to Kh'(L')$. Moreover, we wish this map to be functorial. This makes it possible for us to consider only the case of elementary cobordisms: three Reidemeister moves, and three Mores moves, as illustrated by Figure 3.3.

For an ith Reidemeister move, we define the induced map to be ρ'_{i*} (or its inverse), which is defined in [21] when proving the modified Khovanov homology is independent of the choice of link diagrams.

For a Morse 0- or 2-move, we define the induced map by applying maps $\epsilon : V \to \mathbb{Q}$, and $\iota : \mathbb{Q} \to V$ to the vertices of the cube of resolutions. Here ϵ and ι are given by

$$\epsilon(v_-) = 1 \qquad \epsilon(v_+) = 0 \qquad \iota(1) = v_+.$$

For a More 1-move (or its inverse), we define the induced map by applying m' and Δ' to the vertices of the cube of resolutions.

This completes the construction of the induced map for cobordisms.

3.1.4 The Rasmussen's s-invariant

With the above constructions, we are now able to define Rasmussen's s-invariant. To start with, we recall some properties of Khvanov homology Kh and Lee's modified Khovanov homology Kh'.

Theorem 3.2. *There is a bijective correspondence between the generators of modified Khovanov homology and the possible orientations for L. In particular, $Kh'(L)$ has rank 2^n, where n is the number of components of L.*

We now restrict our attention to a knot K. With the above theorem, we know that there are only two generators for $Kh'(K)$.

Definition 3.3.

$$s_{min}(K) = \min\{s(x)|x \in Kh'(K), x \neq 0\}$$
$$s_{max}(K) = \max\{s(x)|x \in Kh'(K), x \neq 0\}.$$

It turns out that the two generators for Kh' are always different and are adjacent odd integers. To be precise, we have

Proposition 3.4. $s_{max}(K) - s_{min}(K) = 2$.

Proof. See [42]. □

With the above proposition, we can finally define the Rasmussen's s-invariant.

Definition 3.5. We define Rasmussen's s-invariant by

$$s(K) := s_{min}(K) + 1 = s_{max}(K) - 1.$$

We finish this section by quickly going through some properties for the Rasmussen's s-invariant. All of the proofs and be found in [42].

Theorem 3.6. *The Rasmussen's s-invariant descends to a homomorphism from the concordance group $\mathcal{C} = Conc(S^3)$ to $\mathbb{Z}$.*

Theorem 3.7. *The Rasmussen's s-invariant gives a lower bound to the slice genus of a knot. To be precise, we have $|s(K)| \leq 2g_4(K)$. If the knot K is positive as a special case, we have $0 \leq s(K) = g_4(K) = g(K)$.*

Theorem 3.8. *If the knot K is alternating, then the Rasmussen's s-invariant recovers the knot signature $\sigma(K)$.*

Theorem 3.9. *Suppose K_+ and K_- are knots that differ by a single crossing change, from a positive crossing in K_+ to a negative one in K_-. Then $s(K_-) \leq s(K_+) \leq s(K_-) + 2$.*

3.2 The Rasmussen's s Invariant and the Slice Genus

In this section we survey through two exapmples constructed by Piccirillo [36] [37]. The first example proves that the Rasmussen's s-invariant and the slice genus are in fact not trace invariants. The second proves the s-invariant is not a trace invariant, and at the same time proves that the Conway knot is not (smoothly) slice.

3.2.1 Example 1: the Slice Genus

Observe the following family of RBG links L_m and its associated knots K_m and K'_m:
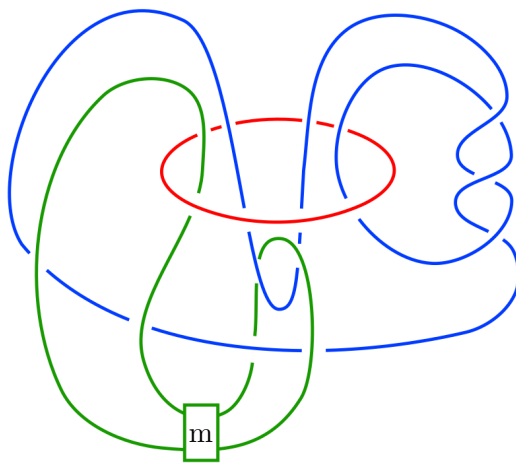
Figure 3.4: The RBG link generating the counterexample
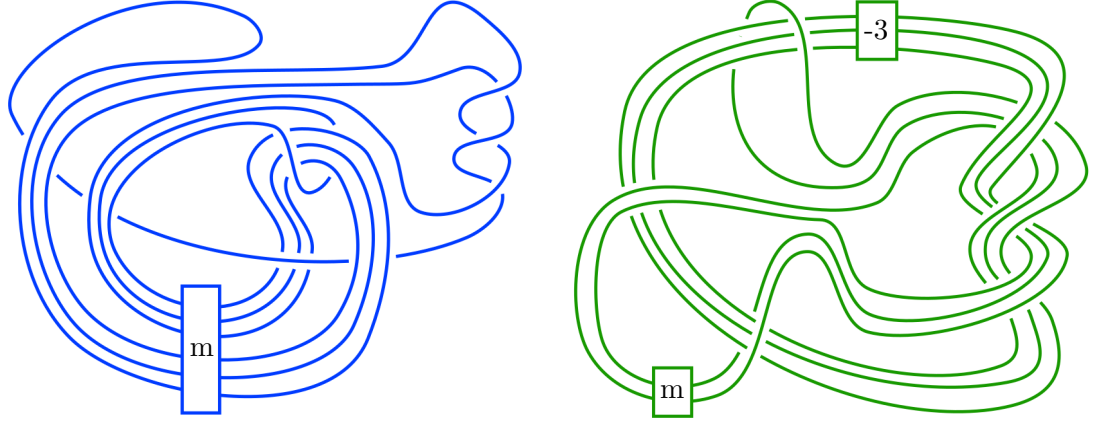
Figure 3.5: Knots related to the RBG link

Note that the RBG link L_m clearly has property U, thus there is a diffeomorphism between the zero traces $X_0(K_m)$ and $X_0(K'_m)$.

Also note that in the RBG link, B and G are split, and G is the unknot, thus the knot K_m, after banding with the bands decorated in the figure, is the unlinked arcs $B \sqcup U \sqcup U$ (in general it would yield $J(G)$). Thus K_m is just concordant to the knot B, i.e. a right handed trefoil knot, and thus has slice genus $g_4(K_m) = 1$ and $s(K_m) = 2$.

On the other hand, we can calculate by KnotJob [43] that the Rasmussen's s-invariant for K'_0 is $s(K'_0) = 4$. By applying Theorem 3.9, we can see that for every $m \leq 0$, we have $2g_4(K'_m) \geq s(K'_m) \geq 4$. This shows the

existence of infinitely pair of knots with diffeomorphic 0-traces but distinct s-invariants and slice genera.

3.2.2   Example 2: The Conway Knot

Another example is Lisa Piccirillo's famous proof of Conway knot is not slice [37].

Take the knot K to be the Conway knot (as described by the left picture of Figure 3.7), where all traditional slice obstructions, Heegaard Floer related invariants (like τ, ν, ϵ, ...) as well as the Rasumussen's s-invariant all vanish. This makes traditional ways to obstruct the Conway knot being slice extremely hard. However, Piccirillo found that we can exploit the s-invariant not being a trace invariant to prove that its zero-trace cannot be embedded in D^4, thus not slice via the trace embedding lemma.

To follow the idea above, we need to find an RBG link with property U such that one of its associated knots is the Conway knot K. To do so, we need the following existence lemma.

Lemma 3.10. *If a knot K has unknotting number 1, then there is an RBG link L such that*

- *$B \cup R \cong B \cup \mu_B, R \cup R \cong G \cup \mu_G$.*

- *The linking number between B and G is zero $lk(B, G) = 0$.*

- *The knot K is one of the associated knots to L.*

Recall that in previous sections, this restriction is denoted as a dualisable link with K as one of its associated knots.

Proof. WLOG, we assume that the unknotting crossing is positive. Then we will first construct an RBG link with one of the associated knots K, and then do some slides to obtain the desired properties.

To define the RBG link, we define (B, b) to be $(K, 0)$. We then define R to be a parallel of B away from the unknotting crossing and as depicted by the leftmost picture of Figure 3.6 near the crossing. Note that R is the unknot by the unknotting assumption. We finally define (G, g) to be the 0-framed meridian of R. It is easy to check this indeed defines an RBG link. Additionally, directly cancelling R and G yields the original knot K.

Then we slide B over R twice as indicated by Figure 3.6. In the rightmost RBG link, observe that both B and G are 0-framed meridians of R. Moreover, we have $lk(B, G) = 0$. This finishes the proof of the lemma.
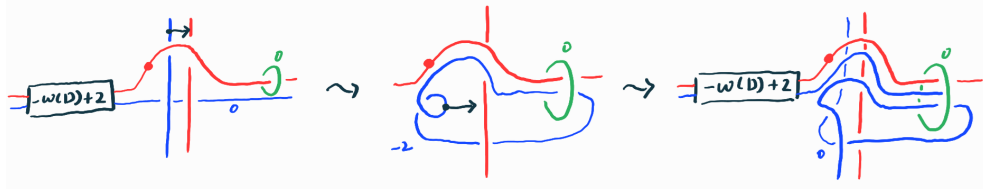
Figure 3.6: Sliding B over R twice yields an RBG link with desired properties

□

With the above lemma, we can follow the construction to obtain the knot K' described by the right picture of Figure 3.7.
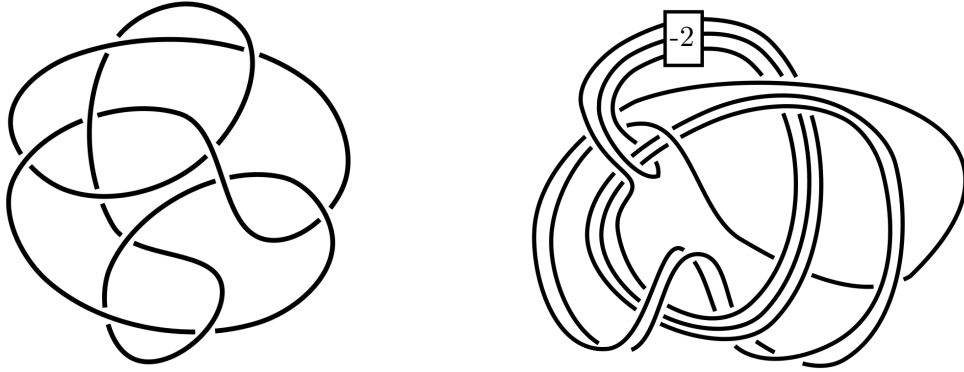
Figure 3.7: Left: The Conway knot. Right: the knot K' whose 0-trace is diffeomorphic to that of the Conway knot.

Now with an easy calculation via KnotJob, we can see that the Rasmussen's s-invariant vanishes for the Conway knot, while the s-invariant for K' is 2. Thus this pair of knots constructs a second counterexample for the s-invariant being a trace invariant, and at the same time, proves that the Conway knot is not slice.

3.3 Heegaard-Floer Theory

In the early 2000s, Peter Ozsváth and Zoltan Szábo introduced a new 3-manifold invariant called the Heegaard Floer Homology [30], defined to be the Lagrangian Floer Homology of the totally real tori related to a Heegaard

splitting. On the knot theory side of the same matter, Ozstháth-Szábo [32] and Rasmussen [41] independently developed knot Floer Homology. In the following years, various concordance invariants were defined based on Heegaard Floer Theory, the most well known ones being the τ-invariant [31] [41], the ν-invariant [34], and the ϵ-invariant [17].

In this part of survey, we focus on the questions on whether the above mentioned concordance invariants are in fact a trace invariant. As a matter of fact, Hayden, Mark, and Piccirillo showed that the ν-invariant is most likely to be a trace invariant, while the τ and ϵ are not [16]. We will start by reviewing some basic definitions and constructions in the Heegaard-Floer theory in this section. In the next section, we will recall the constructions of the concordance invariants and survey through the results of [16].

3.3.1 Preliminaries

Before we define Heegaard Floer homologies, there are a few preliminaries we ned to recall. In this subsection, we will very briefly recall Heegaard splittings and diagrams, symmetric products and totally real tori associated to the Heegaard diagram, holomorphic disks in the tori, and spin^c structures.

Heegaard splittings and Heegaard diagrams A Heegaard splitting (or Heegaard decomposition) is a decomposition of a closed oriented 3-manifold Y into two genus g handlebodies (i.e. a tubular neighbourhood of a wedhe of g circles in 3-space) U_0 and U_1, such that we recover the manifold Y by gluing the two handlebodies via some diffeomorphism of the boundaries $Y \cong U_0 \cup_{\Sigma_g} U_1$. In [44], Singer proved the existence result for Heegaard splittings.

Theorem 3.11. *Let Y be a closed, oriented 3-manifold. The Y admits a Heegaard decomposition.*

Thus we know that the diffeomorphism type of a closed oriented 3-manifold is actually determined by a natural number g, and a self-diffeomorhism of a genus g surface Σ_g. On the other hand, to specify such an automorphism, we only need to specify two sets of attaching circles, defined as follows.

Definition 3.12. Given a genus g hanglebody U with boundary Σ_g, a set of attaching circles $\boldsymbol{\gamma} = (\gamma_1, ..., \gamma_g)$ is a collection of embedded circles in Σ_g such that:

- The curves γ_i are all disjoint from each other.

- The complement $\Sigma_g - \gamma_1 - ... - \gamma_g$ is still connected.

- The curves γ_i bound disjoint embedded disks in the handlebosy U.

With two sets of attaching circles $\boldsymbol{\alpha}$ and $\boldsymbol{\beta}$ given, we can specify a unique automorphism of Σ_g by gluing each α_i to β_i. In this sense, we have a three manifold. Thus, we have the following definition of a Heegaard diagram.

Definition 3.13. A Heegaard diagram $(\Sigma_g, \boldsymbol{\alpha}, \boldsymbol{\beta})$ consists of a genus g handlebody with boundary Σ_g and 2 sets of attaching circles on Σ_g.

Finally we specify the notion of basepoints. An n-pointed Heegaard diagram $(\Sigma_g, \boldsymbol{\alpha}, \boldsymbol{\beta} z_1, ..., z_n)$ consists of a Heegaard diagram $(\Sigma_g, \boldsymbol{\alpha}, \boldsymbol{\beta})$ and a set of n points in $\Sigma_g - \alpha_1 - ... - \alpha_g - \beta_1 - ... - \beta_g$.

Symmetric products and disks in them Recall that our final goal is to apply Lagrangian Floer homology to define a 3-manifold invariant. Thus we need to specify an ambient space and two Lagrangian submanifolds.

Given a Heegaard diagram $(\Sigma_g, \boldsymbol{\alpha}, \boldsymbol{\beta})$, we define the associated ambient space to be the symmetric product $Sym^g(\Sigma_g) = \Sigma_g \times ... \times \Sigma_g / S_g$, which is a $2g$ dimensional manifold. In $Sym^g(\Sigma_g)$, there are two natually embedded g dimensional submanifold $\mathbb{T}_\alpha = \alpha_1 \times ... \times \alpha_g$ and $\mathbb{T}_\beta = \beta_1 \times ... \times \beta_g$ called the totally real tori. It turns out that $Sym^g(\Sigma_g)$ is symplectic and $\mathbb{T}_\alpha$ and $\mathbb{T}_\beta$ are Lagrangian submanifolds.

To actually perform Lagrangian Floer homology, we need to set up some further notations:

- For a pair of intersection points $x, y \in \mathbb{T}_\alpha \cap \mathbb{T}_\beta$, define $\pi_2(x, y)$ to be the set of homotopy classes of Whitney disks connecting x and y, i.e. maps $u : \mathbb{D} \to Sym^g(\Sigma_g)$ such that $u(-i) = x, u(i) = y, u(e_1) \subset \mathbb{T}_\alpha, u(e_2) \subset \mathbb{T}_\beta$, where e_i are the two arcs of the unit disk with positive (or negative resp.) real parts. Note that disk concatenation gives rise to a multiplication operation $* : \pi_2(x, y) \times \pi_2(y, z) \to \pi(x, z)$.

- For a pair of intersection points $x, y \in \mathbb{T}_\alpha \cap \mathbb{T}_\beta$ and a point w in the complement of the curves $\boldsymbol{\alpha}, \boldsymbol{\beta}$, we define the algebraic intersection number $n_w : \pi_2(x, y) \to \mathbb{Z}$ by $n_w(\phi) = \#\phi^{-1}(\{w\} \times Sym^{g-1}(\Sigma_g))$.

- Given $\phi \in \pi_2(x, y)$, define $\mathcal{M}(\phi)$ to be the moduli space of the holomorphic representatives of ϕ. It turns out that after some purturbations, the moduli space is a smooth manifold, and its expected dimension is called the Maslov index. Furthermore, observe that the moduli space

always has an $\mathbb{R}$ action (corresponding to complex automorphisms of the unit disk fixing $\pm i$). Thus we can define the unparameterised moduli space $\widehat{\mathcal{M}}(\phi) := \mathcal{M}(\phi)/\mathbb{R}$.

Spin^c structures We need one last piece of puzzle to define Heegaard Floer homology: the spin^c structures. In the settings of closed oriented three manifolds, we define Spin^c as follows.

Definition 3.14. For two nowhere vanishing vector fields v_1 and v_2, we define them to be homologous if they are homotopic outside some ball B, i.e. $v_1|_{Y-B} = v_2|_{Y-B}$. Finally define Spin$^c(Y)$ to be the space of nowhere vanishing vector fields modulo this equivalence relation.

With the definition above, we can define a map $s_z : \mathbb{T}_\alpha \cap \mathbb{T}_\beta \to$ Spin^c.

Let f be a Morse function related to the fixed Heegaard splitting. Given $x \in \mathbb{T}_\alpha \cap \mathbb{T}_\beta$, it gives g trajectories for ∇f connecting index 1 and 2 critical points for f (one for each pair α_i, β_i). Similarly, z defines a trajectory connecting index 0 and 3 critical points. Deleting the tubular neighbourhoods of these $(g+1)$ trajectories, ∇f defines a nowhere vanishing vector field. This vector field can be extended to a nowhere vanishing vector field on the whole 3-manifold. (Indeed, since vector field has index 0 on the boundary spheres since the deleted trajectories connect critical points of different parities.) By definition, this nowhere vanishing vector field defines a spin^c structure, which we define to be $s_z(x)$.

With all the pieces above, we can simply define the (hatted) Heegaard Floer homology to be the Lagrangian Floer homology of the pair $(\mathbb{T}_\alpha, \mathbb{T}_\beta)$. However, since we will define other variants of Heegaard Floer homologies and knot Floer homologies, we will give a definition explicitly.

3.3.2   The 3-manifold Case

In this section we follow the routine of [30] and survey through constructions of three basic Heegaard Floer homologies for closed 3-manifolds. In most part of this section, we fix our attentions to the case of homology 3-spheres for simplicity, while the general case is very similar but with more technical details, solved also in [30].

The Hatted Heegaard Floer Homology $\widehat{HF}$ We start with the hatted Heegaard Floer homology. Fix a homology 3-sphere Y and a spin^c structure $\mathfrak{t} \in$ spin^c. Given a pointed Heegaard diagram $(\Sigma, \alpha_1, ..., \alpha_g, \beta_1, ..., \beta_g, z)$ of genus $g > 0$, we can define:

- the hatted Heegaard Floer complex $\widehat{CF}(\boldsymbol{\alpha}, \boldsymbol{\beta}, \mathfrak{t})$ to be the free abelian group generated by points $x \in \mathbb{T}_\alpha \cap \mathbb{T}_\beta$ such that $s_z(x) = \mathfrak{t}$.

- relative grading $gr(x, y) = \mu(\phi) - 2n_z(\phi)$. Here ϕ is any element in $\pi_2(x, y)$ and μ is the Maslov index.

- the boundary map $\partial : \widehat{CF}(\boldsymbol{\alpha}, \boldsymbol{\beta}, \mathfrak{t}) \to \widehat{CF}(\boldsymbol{\alpha}, \boldsymbol{\beta}, \mathfrak{t})$ given by

$$\partial x = \sum_{\{y \in \mathbb{T}_\alpha \cap \mathbb{T}_\beta, \phi \in \pi_2(x,y) \mid s_z(y) = \mathfrak{t}, n_z(\phi) = 0\}} c(\phi) \cdot y.$$

  Here $c(\phi)$ denotes the signed number of points in $\widehat{\mathcal{M}}(\phi)$ if $\mu(\phi) = 1$ and zero otherwise.

With the definitions above, it is easy to check that $(\widehat{CF}, \partial)$ indeed defines a chain complex, and thus can yield a homology theory.

Proposition 3.15. $(\widehat{CF}(\boldsymbol{\alpha}, \boldsymbol{\beta}, \mathfrak{t}), \partial)$ *is a chain complex.*

Definition 3.16. Define $\widehat{HF}(\boldsymbol{\alpha}, \boldsymbol{\beta}, \mathfrak{t})$ to be the homology groups of the complex $(\widehat{CF}(\boldsymbol{\alpha}, \boldsymbol{\beta}, \mathfrak{t}), \partial)$.

Finally, we need to show that this homology theory is indeed a 3-manifold invariant and is independent of the pointed Heegaard diagram chosen. The proof can be found in [30].

Theorem 3.17. *Let* $(\Sigma, \boldsymbol{\alpha}, \boldsymbol{\beta}, z)$ *and* $(\Sigma', \boldsymbol{\alpha'}, \boldsymbol{\beta'}, z')$ *be two pointed Heegaard diagrams for* $(Y, \mathfrak{t})$. *Then the Heegaard Floer Homology groups* $\widehat{HF}(\boldsymbol{\alpha}, \boldsymbol{\beta}, \mathfrak{t})$ *and* $\widehat{HF}(\boldsymbol{\alpha'}, \boldsymbol{\beta'}, \mathfrak{t})$ *are isomorphic.*

Thus we can define $\widehat{HF}(Y, \mathfrak{t})$ as $\widehat{HF}(\boldsymbol{\alpha}, \boldsymbol{\beta}, \mathfrak{t})$.

The full Heegaard Floer Homology HF^∞ In the previous construction, we restrict our attentions to disks that do not cross the basepoint. In this section, we loosen the restriction and consider all disks (possibly crossing the basepoint). Similarly, we can define

- $CF^\infty(\boldsymbol{\alpha}, \boldsymbol{\beta}, \mathfrak{t})$ to be the free abelian group generated by pairs $(x, i) \in (\mathbb{T}_\alpha \cap \mathbb{T}_\beta) \times \mathbb{Z}$ such that $s_z(x) = t$.

- relative grading $gr((x, i), (y, j)) = gr(x, y) + 2i - 2j$.

- the boundary map $\partial : CF^\infty(\boldsymbol{\alpha}, \boldsymbol{\beta}, \mathfrak{t}) \to CF^\infty(\boldsymbol{\alpha}, \boldsymbol{\beta}, \mathfrak{t})$ given by

$$\partial(x, i) = \sum_{y \in \mathbb{T}_\alpha \cap \mathbb{T}_\beta} \sum_{\phi \in \pi_2(x,y)} c(\phi) \cdot (y, i - n_z(\phi)).$$

With the above definitions, CF^∞ is again a chain complex, and the correspondingly defined HF^∞ is again independent of the Heegaard splitting.

There is an alternate yet equivalent construction of CF^∞ and HF^∞, defined as follows. We define

- $CF^\infty(\boldsymbol{\alpha}, \boldsymbol{\beta}, t)$ to be the free abelian group generated by $x, i \in \mathbb{T}_\alpha \cap \mathbb{T}_\beta$ such that $s_z(x) = t$ over the ring $\mathbb{Z}[U, U^{-1}]$.

- relative grading as in the "hat" case, while U decreases the grading by 2.

- the boundary map $\partial : CF^\infty(\boldsymbol{\alpha}, \boldsymbol{\beta}, \mathfrak{t}) \to CF^\infty(\boldsymbol{\alpha}, \boldsymbol{\beta}, \mathfrak{t})$ given by

$$\partial x = \sum_{y \in \mathbb{T}_\alpha \cap \mathbb{T}_\beta} \sum_{\phi \in \pi_2(x,y)} c(\phi) \cdot U^{n_z(\phi)} \cdot y.$$

The resulting complex and homology are obviously equivalent to CFK^∞ and HFK^∞.

Remark: This alternative construction can be easily generated to the case with k base points. This is done by chaning the generating ring to $\mathbb{Z}[U_1, U_1^{-1}, ..., U_k, U_k^{-1}]$ and add intersection number restrictions to the summation as before.

The signed Heegaard Floer Homology $HF^\pm$ Define $CF^-(\boldsymbol{\alpha}, \boldsymbol{\beta}, \mathfrak{t}) \subset CF^\infty(\boldsymbol{\alpha}, \boldsymbol{\beta}, \mathfrak{t})$ to be the subgroup freely generated by pairs (x, i) such that $i < 0$. Similar to the "infinity" version, there is an alternate construction: the construction is exactly as the alternative construction described in the previous section except that the generating ring is changed from $\mathbb{Z}[U, U^{-1}]$ to $\mathbb{Z}[U]$.

Define $CF^+(\boldsymbol{\alpha}, \boldsymbol{\beta}, \mathfrak{t})$ to be the quotient group $CF^\infty(\boldsymbol{\alpha}, \boldsymbol{\beta}, \mathfrak{t})/CF^-(\boldsymbol{\alpha}, \boldsymbol{\beta}, \mathfrak{t})$.

Remark: As before, the above definition can also be easily generated to the multi-basepoint scenario.

Note that the subgroup $CF^-(\boldsymbol{\alpha}, \boldsymbol{\beta}, \mathfrak{t})$ is in fact a subcomplex of $CF^\infty(\boldsymbol{\alpha}, \boldsymbol{\beta}, \mathfrak{t})$. Thus we have the following short exact sequence of chain complexes:

$$0 \to CF^-(\boldsymbol{\alpha}, \boldsymbol{\beta}, \mathfrak{t}) \xrightarrow{\iota} CF^\infty(\boldsymbol{\alpha}, \boldsymbol{\beta}, \mathfrak{t}) \xrightarrow{\pi} CF^+(\boldsymbol{\alpha}, \boldsymbol{\beta}, \mathfrak{t}) \to 0.$$

Now we can define the signed Heegaard Floer Homology. As before, we again know that this version of the Heegaard Floer Homology is independent of the pointed Heegaard splitting chosen.

Definition 3.18. Define $HF^{\pm}(\boldsymbol{\alpha}, \boldsymbol{\beta}, \mathfrak{t})$ to be the homology groups of the complex $(CF^{\pm}(\boldsymbol{\alpha}, \boldsymbol{\beta}, \mathfrak{t}), \partial)$.

Theorem 3.19. *Let* $(\Sigma, \boldsymbol{\alpha}, \boldsymbol{\beta}, z)$ *and* $(\Sigma', \boldsymbol{\alpha}', \boldsymbol{\beta}', z')$ *be two pointed Heegaard diagrams for* $(Y, \mathfrak{t})$. *Then the Heegaard Floer Homology groups* $HF^{\pm}(\boldsymbol{\alpha}, \boldsymbol{\beta}, \mathfrak{t})$ *and* $HF^{\pm}(\boldsymbol{\alpha}', \boldsymbol{\beta}', \mathfrak{t})$ *are isomorphic.*

Thus we can define $HF \pm (Y, \mathfrak{t})$ as $HF^{\pm}(\boldsymbol{\alpha}, \boldsymbol{\beta}, \mathfrak{t})$.

3.3.3 Knot Floer Homology

On the side of knot theory, we have a (series of) homology theories very closely related to the 3-manifold version of Heegaard Floer theories. In this section, we follow the routines of [24] to recall the constructions of several basic knot Floer homology theories.

Given a two-pointed Heegaard diagram $(\Sigma, \boldsymbol{\alpha}, \boldsymbol{\beta}, z, w)$ for S^3, we can associate a knot in the following way. We connect z and w by a curve a in $\Sigma - \alpha_1 - ... - \alpha_g$, and similarly connect z and w by a curve b in $\Sigma - \beta_1 - ... - \beta_g$. By pushing a (resp. b) in to the handlebody U_0 (U_1, resp.), we get a knot $K \subset S^3$.

We wish to reverse the above procedure and associate a Heegaard splitting for each knot $K \subset S^3$. The following theorem says that we can.

Theorem 3.20. *Every knot can be represented by a two-pointed Heegaard diagram.*

Proof. We first find a height function h for the knot K with only two critical points A and B, adjusted such that $h(A) = 0$ and $h(B) = 3$. Next we extend the height function to a self-indexing Morse function $\tilde{h}$ on S^3, adjusted such that the index 1 and 2 critical points are away from the knot K. Then $S^3 = \tilde{h}^{-1}((0, 3/2]) \cup \tilde{h}^{-1}([3/2, 3)])$ defines a Heegaard splitting. Note that the surface $\tilde{h}^{-1}(3/2)$ intersects the knot K transversally at two points, which we takes as the two basepoints z, w needed in the desired two-pointed Heegaard diagram. $\square$

With this theorem, we can construct a two pointed version of Heegaard Floer Homology.

The Hatted Knot Floer Homology $\widehat{HFK}$ The hatted version of knot
Floer homology is exactly the two-pointed version of the "hat" version of
Heegaard Floer homology. Namely, we restrict our attention to disks that
do not cross any basepoint. We find an associated two-pointed Heegaard
splitting $(\Sigma, \boldsymbol{\alpha}, \boldsymbol{\beta}, w, z)$ by the above procedure and define

- $\widehat{CFK}(\boldsymbol{\alpha}, \boldsymbol{\beta}, t)$ to be the free abelian group generated by points $x \in$
  $\mathbb{T}_\alpha \cap \mathbb{T}_\beta$.

- relative grading called **Maslov grading** $M(x) - M(y) = \mu(\phi) -$
  $2n_w(\phi)$. Here ϕ is any element in $\pi_2(x, y)$ and μ is the Maslov in-
  dex.

- relative grading called **Alexander grading** $A(x) - A(y) = n_z(\phi) -$
  $n_w(\phi)$.

- the boundary map $\partial : \widehat{CFK}(\boldsymbol{\alpha}, \boldsymbol{\beta}, t) \to \widehat{CFK}(\boldsymbol{\alpha}, \boldsymbol{\beta}, t)$ given by

$$\partial x = \sum_{\{y \in \mathbb{T}_\alpha \cap \mathbb{T}_\beta, \phi \in \pi_2(x,y) | n_w(\phi) = n_z(\phi) = 0\}} c(\phi) \cdot y.$$

  Here $c(\phi)$ denotes the signed number of points in $\widehat{\mathcal{M}}(\phi)$ if $\mu(\phi) = 1$
  and zero otherwise.

  Note that the above defined boundary map decreases the Maslov index
  by 1 and preserves the Alexander grading.

Again we have the following properties and definitions.

Proposition 3.21. $(\widehat{CFK}(\boldsymbol{\alpha}, \boldsymbol{\beta}, t), \partial)$ *is a chain complex.*

Definition 3.22. Define $\widehat{HFK}(\boldsymbol{\alpha}, \boldsymbol{\beta}, t)$ to be the homology groups of the
complex $(\widehat{CFK}(\boldsymbol{\alpha}, \boldsymbol{\beta}, t), \partial)$.

Proposition 3.23. *The homology HFK is independent of the choice of
associated two-pointed Heegaard diagrams.*

Thus we can define $\widehat{HFK}(K)$ as $\widehat{HFK}(\boldsymbol{\alpha}, \boldsymbol{\beta}, t)$.
Remark: some sources like [24] use the notation $\widetilde{gCFK}$ and $\widetilde{gHFK}$ for
this knot Floer homology.

The signed Heegaard Floer Homology $HFK^{\pm}$ Next we consider the case that we allow disks to cross one of the two base points. In this section, we assume that the crossing of w is allowed. In practice, the resulting homology would be the same if we change the choice of the distinguished basepoint.

Just as the standard signed version of Heegaard Floer homology, there is a similar two-pointed version for knots.

Remark: There is another version of the plus/minus version of knot Floer complex which is introduced in the next subsection. To avoid confusion, the "plus/minus" version of knot Floer complex in this section is denoted as $gCFK^{\pm}$ and in the next section $CFK^{\pm}$.

Similar to the first construction, we first pick a two-pointed Heegaard diagram $(\Sigma, \boldsymbol{\alpha}, \boldsymbol{\beta}, w, z)$ associated to the knot K. We then follow the alternative construction from the standard CF^- construction and define:

- $gCFK^-(\boldsymbol{\alpha}, \boldsymbol{\beta}, t)$ to be the free abelian group generated by $x, i \in \mathbb{T}_\alpha \cap \mathbb{T}_\beta$ over the ring $\mathbb{Z}[U]$.

- Maslov and Alexander grading as in the "hat" version, while U decreases the Maslov grading by 2 and Alexander grading by 1.

- the boundary map $\partial : gCFK^-(\boldsymbol{\alpha}, \boldsymbol{\beta}, \mathfrak{t}) \to gCFK^-(\boldsymbol{\alpha}, \boldsymbol{\beta}, \mathfrak{t})$ given by

$$\partial x = \sum_{y \in \mathbb{T}_\alpha \cap \mathbb{T}_\beta} \sum_{\phi \in \pi_2(x,y), n_z(\phi)=0} c(\phi) \cdot U^{n_w(\phi)} \cdot y.$$

Again, its homology is well defined, invariant of the choice of Heegaard splitting, and is denoted by $HFK^-(K)$.

The filtered complex $\mathcal{F}(K, j) \subset \widetilde{CFK}$ In this section, we are still in the setting of allowing disks to cross one of the two basepoints. However, our endgoal here is to construct a filtered Floer complex instead of a Floer homology.

Again we pick a doubly pointed Heegaard splitting assocoiated to the knot K and we define

- $\widetilde{CFK}(\boldsymbol{\alpha}, \boldsymbol{\beta}, t)$ to be the free abelian group generated by $x, i \in \mathbb{T}_\alpha \cap \mathbb{T}_\beta$ over the ring $\mathbb{Z}$.

- Maslov and Alexander grading as in the "hat" version.

- the boundary map $\partial : \widetilde{CFK}(\boldsymbol{\alpha}, \boldsymbol{\beta}, \mathfrak{t}) \to \widetilde{CFK}(\boldsymbol{\alpha}, \boldsymbol{\beta}, \mathfrak{t})$ given by

$$\partial x = \sum_{y \in \mathbb{T}_\alpha \cap \mathbb{T}_\beta} \sum_{\phi \in \pi_2(x,y), n_w(\phi)=0} c(\phi) \cdot y.$$

- $\mathcal{F}(K, j) \subset \widetilde{CFK}$ to be the subcomplex generated by the intersections points $x \in \mathbb{T}_\alpha \cap \mathbb{T}_\beta$ such that $A(x) \leq j$.

The restriction of Alexander grading on $\mathcal{F}(K, j)$ made $\mathcal{F}$ into a filtered complex:

$$... \subset \mathcal{F}(K, j-1) \subset \mathcal{F}(K, j) \subset \mathcal{F}(K, j+1) \subset ...$$

Remark: The associated graded complex $\oplus_j \mathcal{F}(K,j)/\mathcal{F}(K,j-1)$ is exactly the "hat" version $\widehat{CFK}(K)$

The full knot complex CFK^∞ and $CFK^\pm$ Finally we consider the most general case: we allow disks to cross both base points. And our goal is to combine the previous two construction to build a most complete version.

Similar to the standard "infinity" version of Heegaard Floer Complex, there is an "infinity" version of the knot Floer complex $CFK^\infty(K)$, called the full knot complex. Naturally, there are corresponding "plus/minus" version CFK^∞ of the Floer complex.

Again, we first pick a two-pointed Heegaard diagram $(\Sigma, \boldsymbol{\alpha}, \boldsymbol{\beta}, w, z)$ associated to the knot K, and then follow the alternative construction and define

- $CFK^\infty(\boldsymbol{\alpha}, \boldsymbol{\beta}, \mathfrak{t})$ to be the free abelian group generated by $x, i \in \mathbb{T}_\alpha \cap \mathbb{T}_\beta$ over the ring $\mathbb{Z}[U, U^{-1}]$.

- Maslov and Alexander grading as in the "hat" version, and again U decreases the Maslov grading by 2 and Alexander grading by 1.

- the boundary map $\partial : CFK^\infty(\boldsymbol{\alpha}, \boldsymbol{\beta}, \mathfrak{t}) \to CFK^\infty(\boldsymbol{\alpha}, \boldsymbol{\beta}, \mathfrak{t})$ given by

$$\partial x = \sum_{y \in \mathbb{T}_\alpha \cap \mathbb{T}_\beta} \sum_{\phi \in \pi_2(x,y)} c(\phi) \cdot U^{n_w(\phi)} \cdot y.$$

As in the 3-manifold case, the full knot Floer complex CFK^∞ can be seen as freely generated over $\mathbb{Z}$ by triples $(x, i, j) \in (\mathbb{T}_\alpha \cap \mathbb{T}_\beta) \times \mathbb{Z} \times \mathbb{Z}$ with $A(x) = j - i$. In this sense, i describes the negative of the U power; the triple

(x, i, j) corresponds to the generator $U^{-1}x$; and j describes the Alexander grading.

Note that the full knot complex is a filtered complex. We can either view CFK^∞ as a $\mathbb{Z}$-filtered complex over $\mathbb{Z}[U, U^{-1}]$ indexed by the Alexander grading, or we can use the above correspondence and view CFK^∞ as a $(\mathbb{Z} \oplus \mathbb{Z})$-filtered complex over $\mathbb{Z}$ indexed over i and j.

If we take the second perspective, we can draw the full knot complex pictorially:

- We draw each generator (x, i, j) (or equivalently $U^{-i}x$) as a dot at the coordinate (i, j).

- The differential operator ∂ is described by the arrows. Namely, if we have $\phi \in \pi_2(x, y)$, it will change the horizontal coordinate by $-n_w(\phi)$ and vertical coordinate by $-n_z(\phi)$.

- Note that the Maslov index is NOT shown in the picture.

Example. The following is a picture for the full knot complex for the trefoil knot. The detailed calculation will be done in the next section.
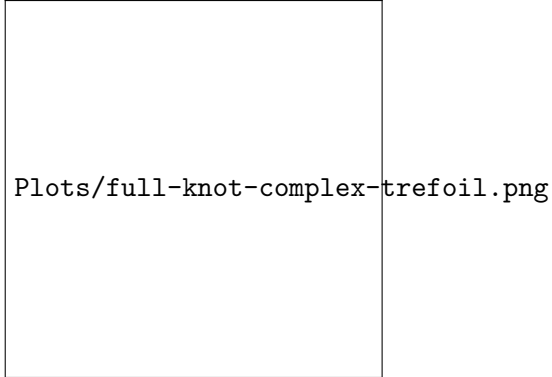
3.4 The τ, ν and ϵ Invariants

In this final section, we will first describe Heegaard Floer homology as 3+1 dimensional TQFTs, namely, how they act on cobordims. Then in the second subsection, we recall the constructions and properties of some Heegaard-Floer theory based concordance invariants: the τ, ν and ϵ invariants. Next we will follow the routine of [16] to survey a counterexample showing that both τ and ϵ invariants are not 0-trace invariants. Finally, we survey the result showing that the ν invariant is most likely a trace invariant.

3.4.1 Heegaard Floer Homology and Cobordisms

In section 3 of this chapter, we explained how the Lee's modified Khoavnov theory behave under cobordisms. I this subsection, we will do the same for Heegaard Floer Theory. To start with, we survey the following main result by Ozaváth-Szabó [30].

Theorem 3.24. *Let W be a connected smooth oriented 4 dimensional cobordism between connected 3-manifold Y_0 and Y_1. fix a spin^c structure $\mathfrak{s}$ for the 4-manifold W. Then there exists an associated map $F^\circ_{W,\mathfrak{s}} : HF^\circ(Y_0, \mathfrak{s}|_{Y_0}) \to HF^\circ(Y_1, \mathfrak{s}|_{Y_1})$. (Here $\circ$ means any Heegaard Floer theory mentioned before, so one of $\{\widehat{}, +, -, \infty\}$.) Additionally, this assignment is functorial, i.e.*

- *If W is the trivial cobordism, then the induced map $F^\circ_{W,\mathfrak{s}}$ is the identity.*

- *Let W_1 be a cobordism from Y_0 to Y_1, W_2 a cobordism from Y_1 to Y_2. Let W denoted the concatenated coborsism, then*

$$F^\circ_{W_2,\mathfrak{s}_2} \circ F^\circ_{W_1,\mathfrak{s}_1} = \sum_{\mathfrak{s} \in spin^c(W), \mathfrak{s}|_{W_i} = \mathfrak{s}_i} F^\circ_{W,\mathfrak{s}}.$$

In other words, this theorem above states that any of the previously surveyed Heegaard Floer theory defines a 3+1 dimensional TQFT.

Next we sketch the construction of the cobordism map in the hatted case. Construction for other cases are similar. Again, since we have funtoriality, we only need to know how the TQFT behaves under the attaching of 1, 2, and 3-handles.

1. Attaching of a 1-handle changes the 3-manifold Y_0 to $Y_0 \# (S^1 \times S^2)$. However, it is easy to see that $\widehat{HF}(S^1 \times S^2) = H_*(S^1) = \langle \theta, \lambda \rangle$, where θ denotes the higher graded element. Then we define the corresponding induced function $\widehat{F}_{W_1} : \widehat{HF}(Y_0) \to \widehat{HF}(Y_0 \# S^1 \times S^2) = \widehat{HF}(Y_0) \otimes \langle \theta, \lambda \rangle$ by $x \mapsto x \otimes \theta$.

2. Attaching a 3-handle is the opposite of attaching a 1-handle. Thus we define the map $\widehat{F}_{W_3} : \widehat{HF}(Y_0 \# S^1 \times S^2) \to \widehat{HF}(Y_0)$ by $x \otimes \theta \mapsto x$ and $x \otimes \lambda \mapsto 0$.

3. Attaching a 2-handle corresponds to doing integral surgery on the 3-manifold. To define the corresponding cobordism map, we need two additional definitions: triple Heegaard-diagrams, and triangle maps.

Definition 3.25. A genus g triple Heegaard diagram associated to 3-manifolds Y_0 and Y_1 is a quadruple $(\Sigma, \boldsymbol{\alpha}, \boldsymbol{\beta}, \boldsymbol{\gamma})$ such that

(a) $(\Sigma, \boldsymbol{\alpha}, \boldsymbol{\beta})$ is a genus g Heegaard Diagram for Y_0.

(b) $(\Sigma, \boldsymbol{\alpha}, \boldsymbol{\gamma})$ is a genus g Heegaard Diagram for Y_1.

(c) Each γ_i and β_i are isotopic (with two intersection points) for each $i < g$, and γ_g intersects β_g at one point.

The following diagram gives a first example of a trigle Heegaard diagram.
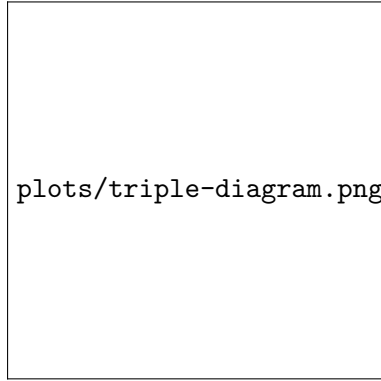
It is easy to see that if Y_0 and Y_1 are related by an integral surgery, then there exists a triple diagram associated to the pair (Y_0, Y_1). To construct a map between them, we need the following definition.

Definition 3.26. Given a triple Heegaard diagram, we consider the three related totally real tori $\mathbb{T}_\alpha, \mathbb{T}_\beta, \mathbb{T}_\gamma$ (or more generally, Lagrangian submanifolds with analogous restrictions), we define the triangle map to be the chain map $F : CF(\mathbb{T}_\alpha, \mathbb{T}_\beta) \otimes CF(\mathbb{T}_\beta, \mathbb{T}_\gamma) \to CF(\mathbb{T}_\alpha, \mathbb{T}_\gamma)$ sending

$$x \otimes y \mapsto \sum_z \sum_{\phi \in \pi_2(x,y,z), \mu(\phi)=0} (\#\mathcal{M}(\phi))z$$

,

where the $\pi_2(x, y, z)$ are J-holomorphic triangles defined analogously as before. Moreover, the triangle map descends to the homology level.

With these two definitions, we can now define the cobordism map. By construction, we have $\widehat{HF}(Y_0) = HF(\mathbb{T}_\alpha, \mathbb{T}_\beta)$, $\widehat{HF}(Y_1) = HF(\mathbb{T}_\alpha, \mathbb{T}_\gamma)$, and $HF(\mathbb{T}_\beta, \mathbb{T}_\gamma) = \langle \theta_1, \lambda_1 \rangle \otimes ... \otimes \langle \theta_{g-1}, \lambda_{g-1} \rangle \otimes \langle \theta_g \rangle$. Thus the cobordism map $\widehat{F}_{W_2} : \widehat{HF}(Y_0) \to \widehat{HF}(Y_1)$ is defined by $x \mapsto F(x \otimes \Theta)$, where $\Theta = \theta_1 \otimes ... \otimes \theta_g$.

3.4.2 Definitions and Properties

The τ invariant Given a knot K, recall from the last section that we can construct its filtered complex $\mathcal{F}(K, m)$, which is a natural subcomplex of the hatted complex $\widehat{CF}(S^3)$. Thus we have a sequence of induced maps

$$\iota_K^m : H_*(\mathcal{F}(K, m)) \to H_*(\widehat{CF}(S^3)) = \widehat{HF}(S^3) \cong \mathbb{Z}.$$

Note that when the filtration m is large enough, the map ι_K^m is always an isomorphism. Thus it makes sense for us to give the following definition:

Definition 3.27.

$$\tau(K) := \min\{m \in \mathbb{Z} | \iota_K^m \text{ is non trivial}\}.$$

Next we quickly survey some of its properties. Note that the τ invariant is, in a way, the Heegaard-Floer version of the Rasmussen's s-invariant, so some properties might look very familiar.

Lemma 3.28. *The map τ induces a group homomorphism from $Conc(S^3)$ to $\mathbb{Z}$.*

Lemma 3.29. *The τ invariant gives a lower bound to the slice genus of a knot. To be precise, we have $|\tau(K)| \leq g_4(K)$.*

Lemma 3.30. *If K is an alternating knot, then the $\tau(K) = -\sigma(K)/2$.*

Lemma 3.31. *Suppose K_+ and K_- are knots that differ by a single crossing change, from a positive crossing in K_+ to a negative one in K_-. Then $\tau(K_-) \leq \tau(K_+) \leq \tau(K_-) + 1$.*

There is a 4-dimensional interpretation of the τ invariant.

Lemma 3.32. *Consider the cobordism map $\widehat{F}_{n,m} : \widehat{HF}(S^3) \to \widehat{HF}(S_{-n}^3(K), \mathfrak{s}_m)$ associated to the knot trace. Here $\mathfrak{s}_m \in spin^c$ is the spin^c structure satisfying $\langle c_1(\mathfrak{s}_m), \sigma \rangle - n = 2m$, where σ is a second homology generator for the knot trace. Then,*

- *For $m < \tau(K)$, the map $\widehat{F}_{n,m}$ is nontrivial for all sufficiently large n.*

- *For $m > \tau(K)$, the map $\widehat{F}_{n,m}$ is trivial for all sufficiently large n.*

The ν invariant   For a knot K in S^3, recall that we can construct a full knot complex $CFK^\infty(K)$ over $\mathbb{F} = \mathbb{Z}/2$. Within that, we define the "hook" knot complexes $\{A_s, s \in \mathbb{Z}\}$ by the quotient $\{\max\{i, j - s\} = 0\}$. Moreover, for simplicity, we let $B_s = \{i = 0\}$, which is just the complex $\widehat{CF}(S^3)$. For each s, there is a natural map $v_s : A_s \to B_s$, which is defined by quotient followed by inclusions. Just like the τ invariant case, this map is in fact identity for large enough s. Thus we have the following definition:

Definition 3.33.

$$\nu(K) := \min\{s \in \mathbb{Z} | v_s \text{ is surjective in homology}\}.$$

Note that Since $\widehat{HF}(S^3) \cong \mathbb{F}$, the map $(v_s)_*$ on homology is non-trivial if and only if it is surjective. It is then easy to see that $\nu(K)$ is either equal to $\tau(K)$ or $\tau(K) + 1$. Thus although it is a concordance invariant, the ν invariant is not a homomorphism from $Conc(S^3)$ to $\mathbb{Z}$.

Also note that the ϵ invariant is also closely related to the two invariants. The precise characterisation is given in the next subsection.

Due to the immense similarity between the ν and the τ invariant, we have a similar 4-dimensional characterisation.

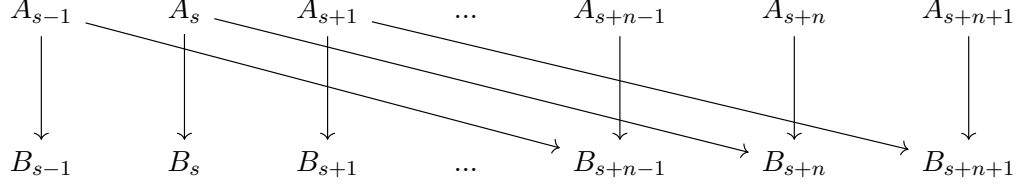**Lemma 3.34.** *Consider the cobordism map $\widehat{F}_s : \widehat{HF}(S^3) \to \widehat{HF}(S_n^3(K), \mathfrak{s}_s)$ associated to the knot trace. Again $\mathfrak{s}_s \in spin^c$ is the $spin^c$ structure satisfying $\langle c_1(\mathfrak{s}_s), \sigma \rangle + n = 2s$. Then*

- *If $|\langle c_1(\mathfrak{s}_s), \sigma \rangle| + n < 2\nu(K)$, then $\widehat{F}_s$ is non-zero.*

- *If $|\langle c_1(\mathfrak{s}_s), \sigma \rangle| + n > 2\nu(K)$, then $\widehat{F}_s$ is zero.*

- *If $|\langle c_1(\mathfrak{s}_s), \sigma \rangle| + n = 2\nu(K)$, then $\widehat{F}_s$ is non-zero if and only if $\epsilon(K) = 0$ and $n \leq 0$.*

Proof. We will only prove the first assertion here.

For the first case, it is proved in [33] that the induced map corresponding to the spin^c stucture $\mathfrak{s}_s$ is exactly given by the inclusion of B_s into the mapping cone of $D_n : \oplus A_s \to \oplus B_s$, described as follows.

We first define the chain map $h_s : A_s \to \{j = s\} \simeq B_s$. Then D_n can be fined by the formula $(s, x) \mapsto (s, v_s(x)) + (s + n, h_s(x))$. Diagrammatically it looks like follows:

64

$$
\begin{array}{ccccccc}
A_{s-1} & A_s & A_{s+1} & \cdots & A_{s+n-1} & A_{s+n} & A_{s+n+1} \\
\downarrow & \downarrow & \downarrow & & \downarrow & \downarrow & \downarrow \\
B_{s-1} & B_s & B_{s+1} & \cdots & B_{s+n-1} & B_{s+n} & B_{s+n+1}
\end{array}
$$

With the result mentioned above, we then observe that the inequality $|\langle c_1(\mathfrak{s}_s), \sigma \rangle| + n < 2\nu(K)$ is equivalent to $-\nu(K) + n < s < \nu(K)$. But this means that the homology of B_s is not in the image of v_k or h_k, thus survives in the homology of the mapping cone. Thus the corresponding cobordism map is non-trivial. $\qquad\square$

We will finish the proof of the last two assertions after the recall of the ϵ invariant in the following subsection.

Now we consider the set of integers $\{s \in \mathbb{Z} | \widehat{F}_s \neq 0\}$. This is a (probably empty) interval of integers centered at $n/2$. If the set is non-empty, denote its maximal element by s_{max}. Then the previous lemma has the following corollary.

Corollary 3.35. *If $\widehat{F}_s = 0$ for all $s \in \mathbb{Z}$, then $\nu(K) \leq n/2$ if n even and $\nu(K) \leq (n+1)/2$ if n odd. Otherwise (i.e. s_{max} is defined), we have $s_{max} \leq \nu(K) \leq s_{max} + 1$, with $\nu(K) = s_{max}$ if and only if $\epsilon(K) = \nu(K) = 0$ and $n \leq 0$.*

Proof. If the maps $\widehat{F}_s$ are trivial for all $s \in \mathbb{Z}$, we know from the first assertion of the lemma that $|\langle c_1(\mathfrak{s}), \sigma \rangle| + n \geq 2\nu(K)$ for all spin^c structures $\mathfrak{s}$. However, the chern number $|\langle c_1(\mathfrak{s}), \sigma \rangle|$ is of the same parity as n, thus obtains minimum at 0 or 1 depending on the parity of n. The claim then follows immediately.

On the other hand, if there exists non-trivial map $\widehat{F}_s$, then s_{max} is defined. By conjugation invariance of the cobordism-induced maps, we know that $\langle c_1(s_{max}), \sigma \rangle \geq 0$, and thus by the second assertion of the lemma, we have $s_{max} \leq \nu(K)$. In the meantime, since $\widehat{F}_{s_{max}+1} = 0$ by construction, we have $s_{max} + 1 \geq \nu(K)$ by the first assertion of the lemma.

Finally we find consitions for equality. We know by definition that if $\nu(K) = s_{max}$, then the map $\widehat{F}_{\nu(K)} \neq 0$. Conversely, if $\widehat{F}_{\nu(K)} \neq 0$, then $\nu(K) \leq s_{max}$. However, the bound we just established ensures $\nu(K) \geq s_{max}$. Thus $\nu(K) = s_{max}$ if and only if $\widehat{F}_{\nu(K)} \neq 0$, which we know is also equivalent to $\epsilon(K) = \nu(K) = 0$ and $n \leq 0$ thanks to the last assention of the lemma above. $\qquad\square$

The ϵ invariant In [17], J. Hom defined the ϵ invariant using the difference in 4-dimensional characterisations between the τ and the ν invariant. To be specific, we define:

Definition 3.36. $\quad\bullet$ If $\nu(K) = \tau(K) + 1$ and $\nu(-K) = \tau(-K)$, then $\epsilon(K) = -1$.

$\quad\bullet$ If $\nu(K) = \tau(K)$ and $\nu(-K) = \tau(-K)$, then $\epsilon(K) = 0$.

$\quad\bullet$ If $\nu(K) = \tau(K)$ and $\nu(-K) = \tau(-K) + 1$, then $\epsilon(K) = 1$.

This characterisation is in fact exhaustive.

Note that the ϵ invariant has the following immediate properties that we survey without proofs.

Lemma 3.37. $\quad$ *1. If K is slice, then $\epsilon(K) = 0$.*

2. If $\epsilon(K) = 0$, then $\tau(K) = 0$.

3. $\epsilon(-K) = -\epsilon(K)$.

4. If K is quasi-alternating, then $\epsilon(K) = sign(\tau(K))$.

5. If $g(K) = |\tau(K)|$, then $\epsilon(K) = sign(\tau(K))$.

6. If $\epsilon(K_1) = \epsilon(K_2)$, then $\epsilon(K_1 \# K_2) = \epsilon(K_1)$. If $\epsilon(K_1) = 0$, then $\epsilon(K_1 \# K_2) = \epsilon(K_2)$.

In particular, the ϵ invariant is a concordance invariant.

Finally, we finish the proof of Lemma 3.34.

Proof of the last two assertions of Lemma 3.34. Now we prove the second case. Thanks to conjugation invariance, we can assume without loss of generality that $\langle c_1(\mathfrak{s}_s), \sigma \rangle + n \geq 2\nu(K)$ $s \geq \nu(K)$. By definition, this means that $H_*(B_s)$ is in the image of v_s in homology. Thus, if there is an element $y_s \in A_s$ such that $v_s(y_s)$ generates homology of $H_*(B_s)$ and $h_s(y_s) = 0$, we can conclude that $H_*(B_s)$ is also in the image of the D_n in homology, and thus the corresponding cobordism map trivial. Thus, the rest of the proof is in search for such an element y_s.

$\quad\bullet$ If $s > -\nu(K)$, then the map h_s is just the zero map. The condition then is easily satisfied.

$\quad\bullet$ If $s \leq \nu(K)$, we take advantage of the following result by Mark-Tosun [28].

Lemma 3.38. *The maps $v_s, h_s : A_s \to B_s$ induce the same map in homology if and only if $s = \epsilon(K) = 0$.*

It is not hard to see that $s = \epsilon(K) = 0$ ensures that $\nu(K) = \tau(K) = 0$, which does not fall in the restrictions of the second assertion. Thus we can safely assume that the maps v_s and h_s do not induce the same surjection $H_*(A_s) \to H_*(B_s)$. Under this assumption, either of the two following cases will happen.

- Exists an element $x \in A_s$ such that $(h_s)_*(x) = 0$ but $(v_s)_*(x) \neq 0$. Then x is the element we are looking for.

- Exists an element $x \in A_s$ such that $(v_s)_*(x) = 0$ but $(h_s)_*(x) \neq 0$. In this case, we can find another element $x' \in A_S$ such that both $(v_s)_*(x') \neq 0$ and $(h_s)_*(x') \neq 0$. Then $x + x'$ is the element we are looking for.

This concludes the proof of the second assertion.

We finally prove the last assertion. Following the discussion from the previous assertion, we can see that if $\epsilon(K) \neq 0$, the the cobordism map is still trivial. Thus we assume $\epsilon(K) = 0$.

If $n > 0$, we pick a generator x_0 for $H_*(B_0) = \mathbb{F}$. Since $\nu(K) = \epsilon(K) = 0$, there exists an element $y_0 \in H_*(A_0)$ such that $(v_0)_*(y_0) = x_0$. By Mark-Tosun's result, we know that $(h_0) * (y_0) = x_n$ is non-trivial. However, we know by definition that $v_n : A_n \to B_n$ is onto (since $n > 0$), and $h_n : A_n \to B$ is trivial (since $\nu(K) = 0$). Thus for any $y_n \in H_*(A_n)$, we know that $(D_n)_*(y_0 + y_n) = x_n$. Thus the inclusion of B_0 into the mapping cone is trivial, and so is the corresponding trivial map.

If $n \neq 0$, again we pick a generator x_0 for $H_*(B_0) = \mathbb{F}$. Again by definition, we know that x_0 is in the image of v_0, and $(h_0) * (y_0) = x_n \in H_*(B_n)$ is non-trivial. However, x_0 is not in the image of h_{-n}, and x_n is not in the image of v_n, as they are zero maps by $-n > -\nu(K) = 0$. Thus, for any element in the image of $(D_n)_*$, if the component in $H_*(B_0)$ is non-trivial, so is the component in $H_*(B_n)$, and in particular, $H_*(B_n) \cap im(D_n) = 0$. Thus for $n < 0$, we know that the inclusion and thus the cobordism map is nontrivial. If $n = 0$, then the mapping cone splits, with one of the subcomplexes the cone of $v_0 + h_0 : A_0 \to B_0$. But this is the zero map since $\mathbb{F} = \mathbb{Z}/2\mathbb{Z}$ by Mark-Tosun's result. Thus the inclusion and thus the cobordism map is non-trivial.
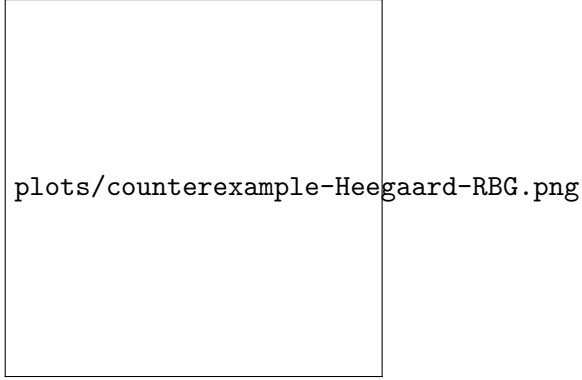
This concludes the proof of lemma 3.34.

$\square$

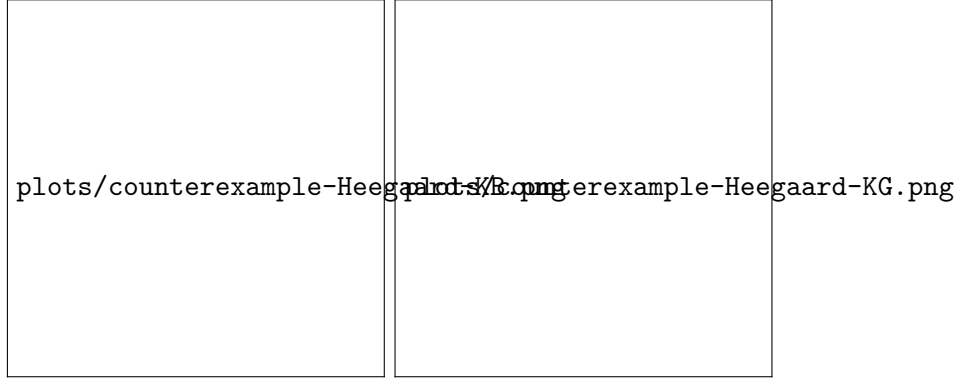Figure 3.8: The *RBG* link generating the counterexample

Figure 3.9: The two knots associated to the RBG link

3.4.3 Counterexamples

The following figures give the RBG link and the associated knots K and K'. It is starightfoward to check that the *RBG* link comes from a dualisable construction, and thus have diffeomorphic 0-traces.

Via the HFK calculator in Snappy [5], once calculates that $\tau(K) = 1$ and $\epsilon(K) = 1$ while $\tau(K') = 0$ and $\epsilon(K') = -1$. This shows that the τ invariant and the ϵ invariants are not trace invariants.

Note that in [6], it is disproved that $\mathrm{rk}\widehat{HFK}(K)(\mathrm{mod}\ 8)$ is not a concordance invariant. It is also conjectured that $\mathrm{rk}\widehat{HFK}(K)(\mathrm{mod}\ 4)$ is indeed a concordance invariant. This same counterexample proves that $\mathrm{rk}\widehat{HFK}(K)(\mathrm{mod}\ 8)$ is also not a trace invariant (since $\mathrm{rk}\widehat{HFK}(K) = 35$, and $\mathrm{rk}\widehat{HFK}(K') = 31$).

Whether or not $\mathrm{rk}\widehat{HFK}(K)(\mathrm{mod}\ 4)$ is a trace invariant is still open.

3.4.4 The ν-invariant is a Trace Invariant

Finally, we will follow the proof from [16] to show that the ν invariant is most likely a trace invariant. To be specific, we will survey the proof of the following theorem.

Theorem 3.39. *If the oriented knot traces $X_n(K)$ and $X_n(K')$ are diffeomorphic, then $\nu(K) = \nu(K')$, except possibly if $n < 0$ and $\{\nu(K), \nu(K')\} = \{0, 1\}$.*

Proof for Theorem 3.39. We first note that a knot trace $X := X_n(K)$ determines the integral framing n and the integer (or not-defined) s_{max}. By changing the orientation of the knot trace, we can also obtain an integer s'_{max}. Thus we reduce the study of an oriented smooth manifold to the study of the three values n, s_{max}, and s'_{max}.

Now we split the problem into three cases:

1. Case 1: s_{max} is defined. We wish to apply Corollary 3.35 to determine the value of $\nu(K)$.

   - If $n > 0$ or $s_{max} \neq 0$, by Corollary 3.35, we know that $\nu(K) = s_{max} + 1$.
   - If $n = 0$ and $s_{max} = 0$. We identify $\nu(K)$ by $\epsilon(K)$. Indeed, from Corollary 3.35, we know $\nu(K) = 0$ if $\epsilon(K) = 0$, and $\nu(K) = 1$ if $\epsilon(K) \neq 0$. However, the two cases can be distinguished by s'_{max}.
     (a) If $\epsilon(K) = 0$, then $\epsilon(-K) = \nu(-K) = 0$. Applying the last assertion of lemma 3.34, we know that $s'_{max} = 0$ and in particular, s'_{max} is defined.
     (b) If $\epsilon(K) \neq 0$, then $\epsilon(-K) \neq 0$ and $\nu(-K) = 0$. Then the last assertion of lemma 3.34 ensures that s'_{max} is not defined.

2. Case 2: s'_{max} is defined. We split the problem into two sub-cases.

   - If $s'_{max} \neq 0$, we first determine the value of $|\epsilon(-K)|$. If $\epsilon(-K) = 0$, then $\nu(-K) = 0$, and thus by Corollary 3.35, $s'_{max} = 0$, yielding a contradiction. Thus $\epsilon(-K) \neq 0$. Thus it follows that $\nu(-K) = s'_{max} + 1$, and $\nu(K) = -\nu(-K) + 1 = -s'_{max}$.

69

- If $s'_{max} = 0$, then by Corollary 3.35, either $\nu(-K) = s'_{max} = \epsilon(-K) = 0$ or $\nu(-K) = s'_{max} + 1 = |\epsilon(-K)| = 1$. However, in either case, it follows immediately that $\nu(K) = 0$. Note that in this case, we fail to determine $|\epsilon(K)|$.

3. Case 3: neither s_{max} nor s_{max} is defined.

   We first claim that $\epsilon \neq 0$. By contradiction, if $\epsilon(K)$ vanishes, then $\nu(-K) = \epsilon(-K) = 0$, and thus by the last assertion of lemma 3.34, the cobordism map induced by the spin^c structure $\mathfrak{s}'_n$ on $-X_n(K)$ is non-trivial. This yields a contradiction.

   Next if n is an even integer, then by Corollary 3.35, we have the ineuqalities $n/2 + 1 \leq -\nu(-K) + 1 = nu(K) \leq n/2$, yielding a contradiction.

   Thus n is odd. A similar bound gives $(n-1)/2 + 1 \leq -\nu(-K) + 1 = nu(K) \leq (n+1)/2$. This tells us that $\nu(K) = (n+1)/2$.

Finally we study the case of $n < 0$. We reverse the orientation to consider $-K$. The above argument shows that we can determine $\nu(-K)$. However, in all but one case, $|\epsilon(-K)|$ is determined, and thus so is $\nu(K)$. The problem occurs at $\nu(-K) = 0$, where we know $\nu(K) \in \{0, 1\}$. This proves the last bit of the theorem

We conclude the proof of the theorem by the following table:

| Correspondence between $\{s_{max}, s'_{max}, n\}$ and $\nu(K)$ and $|\epsilon(K)|$ |
s_{max}	s'_{max}	n	$\nu(K)$	$|\epsilon(K)|$
$\neq 0$			$s_{max} + 1$	1
defined		> 0	$s_{max} + 1$	1
0	defined	0	0	0
0	undefined	0	1	1
undefined	0	> 0	0	???
undefined	undefined	odd	$(n+1)/2$	1
	$\neq 0$		$-s'_{max}$	1
	defined	< 0	$-s'_{max}$	1
0	undefined	< 0	???	???

$\square$

Bibliography

[1] Selman Akbulut and Kouishi Yasui, *Corks, plugs, and exotic structures* (2008).

[2] Stefan Behrens, Boldisár Kalmár, Min Hoon Kim, Mark Powell, and Arunima Ray, *The disk embedding theorem*, 2021.

[3] Steven Boyer, *Simply-Connected 4-Manifolds with a given Boundary* (1986).

[4] W. R. Brakes, *Manifolds with multiple knot-surgery descriptions* (1980).

[5] Marc Culler, Nathan M. Dunfield, Matthias Goerner, and Jeffrey R. Weeks, *SnapPy, a computer program for studying the geometry and topology of* 3-*manifolds.* Available at `http://snappy.computop.org` (01/08/2022).

[6] Nathan Dunfield, Sherry Gong, Thomas Hockenhull, Marco Marengon, and Michael Willis, *On the rank of knot Floer homology theories and concordance* (2023).

[7] M. H. Freedman and F. Quinn, *Topology of 4-manifolds* (1990).

[8] R. Fintushel and R.Stern, *Knots, links, and 4-manifolds* (1998).

[9] M. H. Freedman, *The topology of four-dimensional manifolds* (1982).

[10] Sergei Gukov, James Halverson, Ciprian Manolescu, and Fabian Ruehle, *Searching for ribbons with machine learning* (2023).

[11] D. Gabai, *Foliations and the topology of 3-manifolds* (1983).

[12] Herman Gluck, *The embedding of two-spheres in the Four-sphere* (1961).

[13] Robert E. Gompf, *An infinite set of exotic* $\mathbb{R}^4$*'s* (1985).

[14] _____, *Infinite order corks* (2017).

[15] Robert E. Gompf and András I. Stipsicz, *4-Manifolds and Kirby Calculus*, 1999.

[16] Kyle Hayden, Thomas E. Mark, and Lisa Piccirillo, *Exotic Mazur manifolds and knot trace invariants* (2019).

[17] Jennifer Hom, *The knot Floer complex and the smooth concordance group* (2011).

[18] Kyle Hayden and Lisa Piccirillo, *The trace embedding lemma and spinelessness* (2019).

[19] Mikhail Khovanov, *A categorification of the Jones polynomial* (2000).

[20] Daniel Kasprowski, Mark Powell, and Arunima Ray, *Counterexamples in 4-manifold topology* (2022).

[21] Eun Soo Lee, *Khovanov's invariants for alternating links* (2002).

[22] P. Lisca and G. Matíc, *Stein 4-manifolds with boundary and contact structures*, 1998.

[23] R. Lashof and L. Taylor, *Smoothing theory and Freedman's work on four-manifolds*, 1984.

[24] Ciprian Manolescu, *An Introduction to Knot Floer Homology* (2016).

[25] C. Manolescu, M. Marengon, S. Sarkar, and M. Willis, *A generalization of Rasmussen's invariant, with applications to surfaces in some four-manifolds* (2019).

[26] A. N. Miller and Lisa Piccirillo, *Knot traces and concordance* (2018).

[27] Ciprian Manolescu and Lisa Piccirillo, *From zero surgeries to candidates for exotic definite four-manifolds* (2021).

[28] Thomas E. Mark and Bülent Tosun, *Naturality of Heegaard Floer invariants under positive rational contact surgery* (2018).

[29] Kai Nakamura, *Trace Embeddings from Zero Surgery Homeomorphisms* (2022).

[30] Peter Ozsváth and Zoltan Szábo, *Holomorphic disks and topological invariants for closed three-manifolds* (2003).

[31] _____, *Knot Floer homology and the four-ball genus* (2003).

[32] _____, *Holomorphic disks and knot invariants* (2004).

[33] _____, *Knot Floer homology and integer surgeries* (2007).

[34] _____, *Knot Floer homology and rational surgeries* (2011).

[35] J. K. Osoinach, *Manifolds obtained by surgery on an infinite number of knots in S^3* (2006).

[36] Lisa Piccirillo, *The Conway knot is not slice* (2018).

[37] _____, *Shake genus and slice genus* (2019).

[38] Qianhe Qin, *An RBG construction of integral surgery homeomorphisms* (2023).

[39] Frank Quinn, *Ends of maps. III* (1982).

[40] _____, *Isotopy of 4-manifolds* (1986).

[41] Jacob Rasmussen, *Floer homology and knot complements* (2003).

[42] _____, *Khovanov homology and the slice genus* (2004).

[43] Dirk Schütz, *KnotJob*. Available at `https://www.maths.dur.ac.uk/users/dirk.schuetz/knotjob.html` (01/06/2023).

[44] James Singer, *Three-dimensional manifolds and their Heegaard diagrams* (1933).

[45] Friedhelm Waldhausen, *Heegaard-Zerlegungen der 3-Sphäre* (1968).

[46] Kouichi Yasui, *Corks, Exotic 4-manifolds and knot Concordance* (2017).